University of Exeter coursework header sheet

ECMM102 Group Project (Meng) (A, TRM1+2 2014/5)

018372

1015549

600021651

Coursework: I2

Submission Deadline: Thu 30th Apr 2015 12:00

Personal tutor: Dr Christopher Smith

Marker name: Gavin Tabor

Word count: 11751

By submitting coursework you declare that you understand and consent to the University policies regarding plagiarism and mitigation (these can be seen online at www.exeter.ac.uk/plagiarism, and www.exeter.ac.uk/mitigation respectively), and that you have read your school's rules for submission of written coursework, for example rules on maximum and minimum number of words. Indicative/first marks are provisional only.

First marker's comments

Indicative mark

Second marker's comments

Second mark

Moderator's comments

Agreed mark

I2 Report

The Effects of Topography on Wind Flow

Joshua Mullins

2015

4th year MEng Group Project

I certify that all material in this thesis that is not my own work has been identified and that no material has been included for which a degree has previously been conferred on me.

Signed 

College of Engineering, Mathematics, and Physical Sciences
University of Exeter

I2 Report

ECMM102

Title: The Effects of Topography on Wind Flow
Word count: 11751
Number of pages: 40

Date of submission: Wednesday, 29 April 2015

Student Name: Joshua Mullins
Programme: Mechanical Engineering
Student number: 600021651
Candidate number: 018372

Supervisor: Dr. Gavin Tabor

Abstract

This project was undertaken as a contribution to the group project '*Research into the Causes and Effects of Aeroelastic Flutter on Long Span Bridge Structures'*. This project used the Humber Bridge as a case study, and involved structural analysis and fluid dynamics techniques.

The aim of this project was to investigate the effect that topographical features have on wind flow. Boundary conditions were specified to correctly model the Atmospheric Boundary Layer (ABL) and were validated in a steady-state simulation of flow over the Askervein Hill. An accurate representation of terrain local to the Humber Bridge was produced in STL format using Lidar data. The computational fluid dynamics (CFD) code, OpenFOAM, was used for analysis. Transient simulations took place using the standard k-epsilon model to determine the effect topography had on wind flow near the Humber Bridge. Wind speed-up over topographic features ranged from -0.325 to 0.15. Turbulent kinetic energy of the flow was increased at the ground and flow separation was observed over topographic features. A flow profile from the terrain study was used as an inlet condition in a case study of flow over the Humber Bridge deck. The effect of this flow over the deck was negligible, in comparison to a standard inlet condition. It was determined that to accurately model flow in the ABL, a variable surface roughness is required to model topographical features within a fluid domain. Time marching solvers were required to simulate flow over complex terrain that would include transient flow components. While the effect of topography on wind flow was quantified, wind tunnel data or field experiments are required in future work for validation of the numerical results provided by CFD.

Keywords: *Humber Bridge, Turbulence Modelling, OpenFOAM, Topography, Atmospheric Boundary Layer*

Acknowledgements

Many thanks to Dr. Gavin Tabor for his supervision and advice on OpenFOAM and CFD throughout the course of this project. Thanks also to Shenan Grossberg for showing the CFD subgroup how to use the HPC cluster, Callisto.

Table of contents

1. Introduction and Background 1
1.1. Aims 1
1.2. Objectives 2
2. Literature Review 3
2.1. Wind Engineering 3
2.2. CFD for Wind Flow over Complex Terrain 4
2.2.1. Askervein Hill Experiment 4
2.2.2. CFD Modelling of the Atmospheric Boundary Layer 6
3. Theoretical Background and Methodology 7
3.1. Computational Fluid Dynamics 8
3.1.1. Turbulence Modelling 9
3.1.2. Reynolds Averaged Navier Stokes Equations 10
3.1.3. LES and DES Modelling 10
3.1.4. Near Wall Meshing 11
3.2. Topographical Data Conversion 12
3.2.1. SnappyHexMesh 13
3.3. CFD Simulations 14
3.3.1. Boundary Conditions 15
3.3.2. Surface Roughness and K-epsilon Parameters 16
3.4. Askervein Hill Validation Case 16
3.5. Humber Bridge Terrain 18
3.6. Effect of Flow upon Bridge Deck 20
4. Computational Results and Discussion 22
4.1. Askervein Hill Results 22
4.1.1. Analysis and Discussion 23
4.2. Humber Bridge Results 25

4.2.1. Analysis and Discussion 27
4.3. Bridge Deck Results 30
4.3.1. Analysis and Discussion 31
5. Conclusions 32
5.1. Conclusions 32
5.2. Future Work 33
6. Project Management 34
6.1. Project Management 34
6.2. Project Risk Assessment 35
6.3. Project Cost and Sustainability Considerations 35
7. Contribution to Group Functioning 36
7.1. CFD Subgroup 36
7.2. Fluid-Structure Interaction 37
8. References 37

1. Introduction and Background

As long span bridges become more efficient in design, greater consideration must be given to their response to wind flow. Suspension bridges may be lower in mass and less stiff than other designs making the structure susceptible to wind induced structural vibrations [1]. Bridge designs are typically analysed by testing scale models within Boundary Layer Wind Tunnels (BLWT). Testing can be used to determine the fluid-structure interaction and dynamic response of a bridge, such as flutter, buffeting, and vortex-shedding induced vibration. Topography and man-made features are included in testing to replicate real world conditions.

Computational Fluid Dynamics (CFD) is a computational method used for the analysis of simulated fluid flow. Most fluid flows are turbulent, so much of the field of CFD deals with resolving and modelling turbulence. In comparison to BLWT testing, it is relatively inexpensive and has several advantages; it can be used to derive data at any point in a fluid flow without necessitating additional instrumentation, changes can be made virtually to simulate physical changes quickly and visualisation of complex fluid flow (e.g. turbulence) is possible. These advantages over wind tunnel testing are a prime motivator for the project and make it a suitable approach in wind engineering analysis and design.

One of the main objectives for the group project *'Research into the Causes and Effects of Aeroelastic Flutter on Long Span Bridge Structures'* [2] was to simulate wind flow over the Humber Bridge to determine a vortex shedding frequency. This study included the parameters of terrain and the atmospheric boundary layer (ABL), upon which this project is based. The other main objective was to analyse the structure of the bridge to determine its vibrational response. Data from structural and CFD models was combined to investigate fluid-structure interaction, relating the frequency of vortex shedding to the natural frequencies of the bridge. This data was used to determine the circumstances at which the bridge is most affected by vortex-induced vibration. This was with the aim of determining wind conditions at which the vibrational response of the bridge might necessitate its temporary closure.

1.1. Aims

The main of aim of this project was to perform CFD simulation of the ABL over complex terrain. This was performed using OpenFOAM v2.1.0 [3]. Another aim was to quantify the effects of terrain on wind flow, and the resulting effects this had on a bridge deck.

GlobalMapper, SolidWorks, Matlab and MeshLab were used to incorporate realistic terrain and bridge geometry into OpenFOAM.

1.2. Objectives

- To investigate the effect of topography on wind flow
- To assess the effect of turbulent wind flow on the Humber Bridge deck
- To develop a method to integrate topographical data for analysis in OpenFOAM

The deliverables for the individual project were as follows:

- Create fluid domains derived from topographic data with appropriate boundary conditions to accurately simulate the ABL
- Perform CFD simulations of fluid flow over complex terrain and validate the results
- Produce a study on how topography affects wind flow over the Humber Bridge

Several assumptions were made in regards to this project. Wind flow across the terrain was always set perpendicular to the bridge deck. This was because a crosswind flow scenario would be most likely to induce vortex shedding across the bridge deck, which acts as a bluff body. This is in contrast to BLWT testing, where a rotating section is used to simulate wind flow around 360 degrees. In terms of scope, only the effects of local topography on wind flow were studied. As such, fluid flow domains were made up to 3000m×3000m. This was practical, given the span of the Humber Bridge (2100m) and available computational resources. This is in line with the numerical simulation of wind flow using CFD. Meso-scale (2-200km) and large scale (200-2000km) wind flows are dealt with by numerical weather prediction software [4]. To reduce complexity and to improve the quality of CFD meshes, the cables, internal deck structure, and towers of the Humber Bridge were omitted.

The format of this report is as follows; a literature review of work in the field of CFD, simulating wind flow over terrain is presented, a theoretical background and methodology detailing case studies of simulations of wind flow over the Askervein Hill and terrain near the Humber Bridge. The effect of wind profiles (derived from terrain flow simulations) upon a bridge deck was then determined. Results and analysis were determined from numerical simulations. Conclusions and recommendations for future work are presented. The contribution of the work conducted in this report to the overall group project is also detailed.

2. Literature Review

Topography is a field of science involving the study of the shape and size of features of the earth's surface. This project focused upon CFD evaluation of localised topographical (relief, terrain), vegetation and man-made structures together. As a term of reference and for a review of previous work, the reader may be referred to *'Individual Report I1'* [5].

2.1. Wind Engineering

The direct influence of topography on the dynamic wind loading of long span bridges has been studied within the confines of wind tunnels but less so through CFD analysis [6]. There are disadvantages and advantages in using CFD for fluid flow analysis in comparison to wind tunnel testing [7]. Some advantages of CFD are its low cost and quick analysis set-up times. The wind loading chain has been recognised as an approach for evaluating the factors that influence wind loads and responses of buildings and structures (Figure 1). This links the different aspects of wind flow modelled by members of the CFD subgroup.

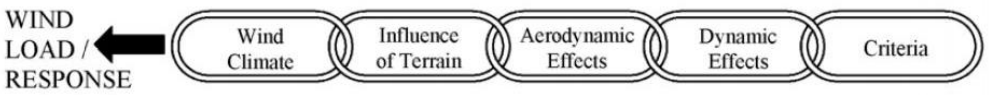

Figure 1. Alan G. Davenport Wind Loading Chain [8]

Davenport et al. [9] showed that the effects of topography are significant when defining design wind loads for long span bridges. In wind tunnel testing of the Roosevelt lake bridge, sheltered areas experienced 40-50% of mean averaged wind speeds compared to free flow areas. This was due to the presence of a dam parallel to the bridge. Local turbulence intensities followed a reverse trend, where areas of low mean wind speed had higher relative turbulence intensities around 25%. Elsewhere, effects of terrain on wind flow were observed, with a mean ±3% variation in velocity and a uniform turbulence intensity of 10%. The dynamic peak lift response of the bridge was found to be proportional to the free stream velocity and the intensity of the turbulence upstream. The mean drag across the deck also varied between areas exposed to high wind velocity and those with low velocity (shielded by the dam upstream). It was observed that vortex shedding over the dam and bridge was eliminated at turbulences of moderate intensities.

2.2. CFD for Wind Flow over Complex Terrain

A characteristic feature of bridges are their locations. They are inherently located between features such as gorges, hills, rivers and bodies of water. Surface roughness, height and distribution of topographical features can increase wind velocity (Figure 2). It can also induce turbulence and cause wind funnelling. Human structures and vegetation also have an effect on wind flow. Urban canyon flow has been shown to cause pressure and velocity fluctuations in near structures and increase turbulent kinetic energy (TKE) of the flow [10]. These effects can cause uncomfortable fluctuating wind flows for pedestrians and may cause bridges to be temporarily closed under adverse weather conditions.

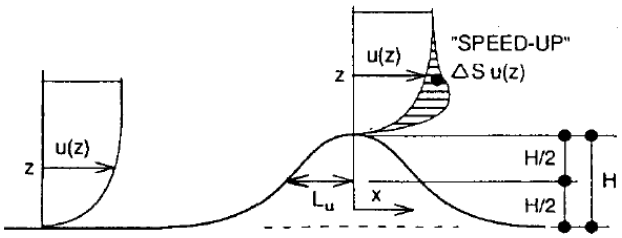

Figure 2. Topographic multiplier and speed-up [11]

2.2.1. Askervein Hill Experiment

CFD has been used to model wind flow over a range of topographical scales, from several km down to single hills. The level of resolution in the topographical data has ranged from 90m of the Shuttle Radar Topography Mission, to high resolution UK Lidar data of 2-0.25m [12]. While many CFD studies on complex terrain have been performed, few authors refer to the method by which complex terrain data has been extracted from sources such as Lidar.

The main issue in modelling wind flow over complex terrain is a lack of experimental data with which to compare results. This is important in order to validate the choice of turbulence model and solver, and determine the accuracy of numerical results. For these reasons, many CFD studies have used two benchmark cases where experimental data is available: the Bolund [13] and Askervein hill experiments [14]. The Askervein hill is a 116m high, elliptical hill, 2000m long by 1000m wide. It is located on the west coast of South Uist, in the Outer Hebrides, Scotland. Between 1982 and 1983 a wind measurement campaign was performed. CFD results for this case are usually compared against a data set taken during a three hour period on October 3rd 1983 when the atmosphere was neutrally stable and a South Westerly wind was blowing at 210°. The reference velocity was measured as 8.9m/s at a height of 10m. Wind speed was

measured along 3 lines using anemometers. Peralta et al. [15] validated the OpenFOAM RANS (Reynolds Averaged Navier Stokes) steady-state solver, *simpleFoam,* for simulating the neutral ABL flow for the Askervein hill case for several two equation turbulence models. The authors developed their own utility 'terrainBlockMesher' to build a structured mesh for the terrain. This produced better boundary layers for the mesh than the native OpenFOAM mesher, *snappyHexMesh* (SHM), at the cost of an increased number of cells. Numerical accuracy was increased, with a smaller percentage difference between experimental data from the Askervein hill experiment than with the SHM. The case used the OpenFOAM ABL inlets. These apply a logarithmic inlet velocity profile for k-epsilon models based upon appropriate boundary conditions for atmospheric wind flow suggested by Richards & Hoxey [16]. The boundary conditions were; a zero gradient pressure outlet, top and sides defined as slip patches and a ground patch with standard wall functions and a constant roughness function. In line with experimental data, the surface roughness height, $z_{0,}$ was defined as 0.03, indicating light vegetation. The simulations had residuals convergence criterion of 1×10^{-5} and it was shown that the RNG k-epsilon model predicted flow over the hill most accurately. This is in contrast to other studies. Gobbi et al. [17], Castro et al. [18] and da Silva [19] indicated no benefit in using the RNG k-epsilon turbulence model, and the conclusion drawn from their results was that the standard k-epsilon model predicted the flow over the Askervein hill most accurately. This discrepancy may be indicative of how different computational meshes affected the results. It could be expected in cases of circulating flow that the RNG model may be more appropriate because it accounts for different scales of turbulent motion and the effect of swirl on turbulence.

Studies on the Askervein hill and complex terrain have been performed using Large Eddy Simulation (LES) [20] and Detached Eddy Simulation (DES) [21]. The motivation in using LES and DES was to improve the accuracy of numerical results, and to capture the wind flow accurately in the leeward side of the Askervein hill. This was problematic with RANS models because they were unable to capture the intermittent flow separation. Turbulence intensity was well predicted in comparison to two equation RANS models. This was expected, given the tendency of these models to over-predict TKE within a flow. Even with a DES simulation, grid convergence was not achieved in these studies. This was shown by the increasing size of a circulation zone in the lee of the hill with increasing mesh refinement. In summary, it was shown that both RANS and LES/DES gave similar predictions for speed-up along the domain, consistent with experimental data. It was deemed acceptable to perform CFD simulations in

this report with transient time-marching simulations using RANS turbulence models. This was decided because RANS models are suitably accurate in predicting flow over terrain, and computationally inexpensive. It also meant that larger meshes, on the order of 1×10^6 cells could be used within a realistic timeframe (days as opposed to weeks). RANS modelling negates the problem of demanding mesh refinement for LES/DES where $y+$ values less than 1 are required. The meshing requirements and small time step required for numerically stable flow over complex terrain at high Reynolds numbers made LES and DES unrealistic options given their high computational cost.

2.2.2. CFD Modelling of the Atmospheric Boundary Layer

The ABL is part of the planetary atmosphere that is directly influenced by the surface of the earth. It is affected by temperature, frictional drag, stratification, surface roughness, pollutants and terrain. It extends from the surface of the earth up to a height of 2000m where there is a free atmosphere. The structure shares similarities to boundary layers of all scales (Figure 3). Within the rough sublayer, the turbulence and mean velocity profiles are highly dependent upon the size and frequency of the roughness and surface features. The ABL is determined to be neutrally stable if the air within it does not experience a buoyancy force when it moves. The ABL is generally modelled in CFD up to the inertial sublayer (500m max). The Coriolis effect is ignored, as it is negligible compared to the effect of terrain on wind flow. In wind engineering applications, buoyancy and stratification effects are ignored and incompressible and dry air properties are used for wind flow.

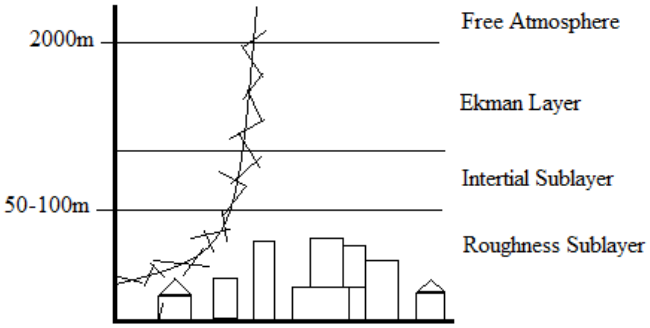

Figure 3. General structure of the ABL

The ABL is generally modelled as a horizontally homogeneous turbulent surface layer, where constant properties are defined tangentially to the surface and variations are only made perpendicular to the surface. In a study by Richards and Norris [22], two equation eddy-viscosity models (k-epsilon, RNG k-epsilon, k-omega) were compared to the LRR Reynolds

stress model (RSM) in calculating pressure on a chimney in atmospheric wind flow. It was shown that the two equation models over-predicted the pressure (and loading) on the windward face of the chimney. The RSM avoided this behaviour, and provided a constant pressure coefficient along the height of the chimney. This study showed that there are certain limitations in turbulence modelling of wind flows. Two equation RANS models assume that turbulent eddies are isotropic and in particular, the k-epsilon model may not be sufficient in capturing the important dynamics of wind flow over complex topography [23]. This is expected, given the purpose of RANS eddy-viscosity models to average all scales of turbulent eddies to a mean turbulence field. In finding pressure forces, a RSM has been suggested to be more accurate, due to its ability to model anisotropic turbulent eddies, account for streamline curvature, and high rotation within a flow [24]. As is typical in CFD, there is a trade-off between numerical accuracy and computational expense. A RSM is considerably more computationally expensive to model a flow, than a two equation turbulence model. In reference to the previously discussed studies on the Askervein hill, the use of the standard k-epsilon models yielded results which were considered accurate. It is a case of diminishing returns to apply a RSM to ABL flow over complex terrain. Instead, it would be more appropriate to switch to DES models, which may be more computationally expensive than RSM, but provide much more accurate results.

It was demonstrated by Krogstad et al. [25] through experimental methods that the surface of a geometry significantly affects the turbulent characteristics of a flow, even when roughness geometries are chosen so as to achieve the same effect on the mean velocity of the flow. Therefore, only CFD simulations that took into account both the geometry and roughness of the earth's surface would accurately reproduce wind flow.

3. Theoretical Background and Methodology

The first step taken in modelling fluid flow over complex terrain was to convert topographical Lidar data to a STereoLithography (STL) format. This was required because the native OpenFOAM polyhedral mesher, SHM, works by snapping from an initial hexahedral mesh to an STL surface. This deliverable was difficult to achieve, as no suitable method for combining data across multiple grid squares (as Lidar data was supplied) existed.

To ensure that numerical results given by CFD simulations could be trusted, a validation study was made using the well documented Askervein hill case. This ensured that boundary

conditions and turbulence models matched the experimental data and that these same conditions could be applied with some confidence in future studies of flow over topography.

Once this method was established, it was determined if there was the possibility to assess the effect of terrain on wind flow, with an aim to determining the resulting effect on the Humber Bridge deck. An initial case was made to explicitly model this, involving a fluid domain with both terrain and the bridge deck. This method was shown to be inaccurate and computationally costly, making it an unsuitable approach. To overcome this problem a study of flow over the terrain near the Humber Bridge was made and velocity profiles extracted. The effect of topography on fluid flow was implicitly derived by applying the extracted velocity flow profiles as initial conditions in a study of a flow over a Humber Bridge deck cross section.

3.1. Computational Fluid Dynamics

CFD is a method to simulate fluid flow using computational methods. Fluids are influenced by viscous and body forces. Fluid behaviour is described by the Navier-Stokes (N-S) equations, a set of five coupled partial differential equations; a continuity equation for conservation of mass, energy equation and 3 dimensional x, y and z momentum equations (Equation 1). Except for a few very simplified cases, the Navier-Stokes equations are too complicated and time consuming to solve analytically. To obtain numerical solutions, CFD codes use the finite volume (FV) method. A solution to fluid flow is made by the creation of a virtual domain. This is represented as a geometric shape, with defined inlet, wall and outlet conditions as parameters for the fluid flow. The domain is discretised into a finite number of volumes (cells). The discretised domain and cells are known as a mesh. From initial conditions the flow can be numerically calculated across the entire domain. This is done iteratively by solving the governing fluid flow equations between each of the cells.

$$\frac{\partial u_i}{\partial t} + \frac{d(u_i u_j)}{\partial x_j} = -\frac{1}{\rho}\frac{\partial p}{\partial x_i} + \frac{\partial}{\partial x_j}\left[v\left(\frac{\partial u_i}{\partial x_j} + \frac{\partial u_j}{\partial x_i}\right)\right] + f_i$$

$$\frac{\partial u_i}{\partial x_i} = 0$$

Equation 1. Incompressible form of the Navier Stokes equations

Where; v is kinematic viscosity, ρ is fluid density, p is pressure, x_i are the components of a Cartesian co-ordinate system, u_i represents velocity components and f is body forces acting on the fluid. For conciseness, the mathematical derivations of the FV method, CFD solution and

discretisation methods will not be covered in this report. These are well documented in literature (*'Computational Fluid Dynamics: A Practical Approach'* [26]).

3.1.1. Turbulence Modelling

Turbulence is defined as chaotic and random motions within a fluid. Turbulent flow can be induced by; bluff bodies, geometric variations, free stream velocity and rough walls in a flow. The point at which turbulence occurs is characterised by the Reynolds number. This dimensionless number represents the ratio between viscous and body forces within a fluid (Equation 2).

$$Re = \frac{inertial\ forces}{viscous\ forces} = \frac{uL}{v}$$

Equation 2. Reynolds Number

Where; u = free stream velocity, L = characteristic length, v = kinematic viscosity of the fluid.

At low Reynolds numbers, body forces are smaller than viscous forces. Naturally occurring turbulence is dissipated and fluid flow generally remains laminar up to Reynolds number of 2300. At high Re (>2300), inertial forces are large enough to magnify disturbances in the fluid, causing a transition to turbulence. The time varying nature of random fluctuations of turbulent fluid flow mean that the equations previously used to describe fluid flow cannot be used. As the velocity fluctuates randomly over time, it is hard to predict. To model this, a mean velocity value is taken and used with a time varying velocity component, $u(t) = \bar{u} + u'(t)$.

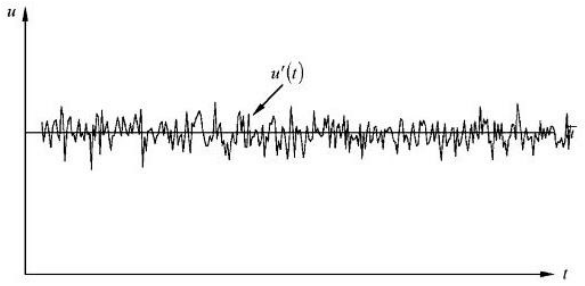

Figure 4. Velocity Fluctuations in Turbulent Flow over Time [26]

This forms the basis for the creation of turbulence models used as approximations to deal with the effect of turbulent fluctuations in the fluid flow (Figure 4). Turbulence can be characterised by eddies which have a length scale and velocity. The kinetic energy of a flow passes down a hierarchy from large to small eddies through the breaking up of large eddies into smaller and smaller ones (energy cascade). At the smallest (Kolmogorov) scale, the remaining kinetic

energy is dissipated as heat. The turbulence model chosen depends upon the size of the turbulent eddies, the solution accuracy desired and the time taken for computation (Figure 5).

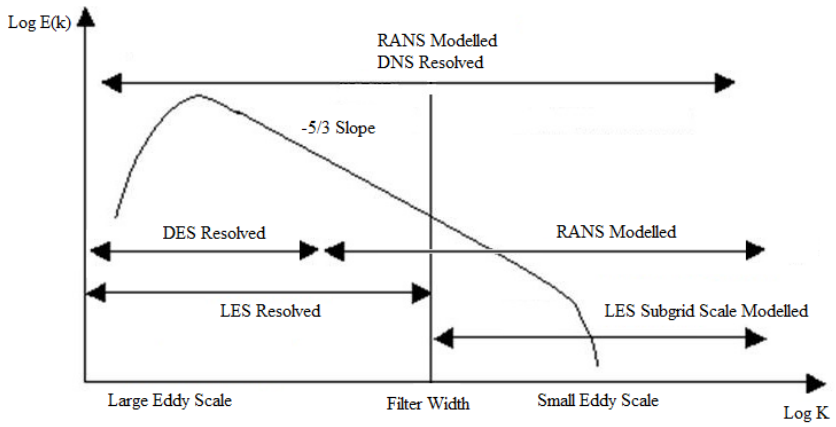

Figure 5. Turbulent energy spectrum and turbulence models used at different eddy scales

3.1.2. Reynolds Averaged Navier Stokes Equations

RANS eddy-viscosity models model turbulent flow by estimating the effect of instantaneous fluctuating turbulence properties upon the mean flow by using time averaged N-S equations. The k-epsilon turbulence model is widely used in complex terrain and wind flows. It averages a turbulent flow using defined values for the TKE (k) along with the rate of energy dissipation (ε) (Equation 3). RANS models are stable and efficient in terms of computation time. However, they average all turbulent length scales, producing a time-averaged field that reduces solution accuracy. In addition, some two equation RANS models fail to predict unsteady characteristics of separated flows [27]. This has presented itself as a limitation in using these models to predict turbulent flows over the terrain where separation occurs in the leeside of relief such as hills [20].

$$k = \frac{3}{2}(U_{ref}T_i)^2 \qquad \varepsilon = C_\mu{}^{3/4}\frac{k^{3/2}}{l} \qquad \omega = \frac{\varepsilon}{C_\mu k} \qquad l=0.07L$$

Equation 3. K-epsilon parameters

Where, L is characteristic length scale, U_{ref} is inlet flow velocity, T_i is turbulent intensity (usually 5-20%), ω=Omega, C_μ=0.09.

3.1.3. LES and DES Modelling

LES explicitly resolves large scale anisotropic eddies and models small scale turbulent eddies. A filter is applied and all smaller eddies in this sub grid scale are decomposed and averaged. The filter width is defined by cell size. Detached eddy simulation (DES) has been used to model

turbulent atmospheric flows. It is useful where high Reynolds number flows need to be solved, where LES can be unsuitable due to costly meshing requirements. DES models are hybrids between RANS and LES. An LES-type model is used to directly solve large scale eddies in the majority of the flow while RANS-type models are used to capture turbulent conditions near walls. It solves the problems that RANS is unable to resolve all the turbulent scales accurately while reducing the high computational cost of LES modelling.

3.1.4. Near Wall Meshing

It is important in CFD to ensure that the set of finite volumes in a mesh are of sufficient quality and resolution. This contributes to producing numerically accurate results. As ever, there is a trade-off between numerical accuracy and computational cost, as high resolution meshes take longer to solve. It is good practice to increase mesh resolution at points of interest and where boundary layers form (Figure 6). Walls have a large influence on the behaviour of turbulent flow. In the literature cases reviewed, the mesh near the surface of the terrain and leeward sides of interesting topographical features was highly refined. Meshing requirements in near wall regions is dependent upon the turbulence model used. LES fully resolves boundary layer flow and so requires values of $y^+ < 1$ near walls. In RANS modelling, values of $y^+ > 11.6$ are required because wall functions are used to model the flow properties near the wall. To use wall functions, the cell centre of the first cell adjacent to the wall should be within the log-law region of the boundary layer (Figure 6). To satisfy this condition, $20 < y^+ < 300$ are generally accepted, although there is technically no upper limit for y^+ values in RANS modelling [28]. Equation 4 shows how a CFD solver calculates y^+ values. These values are dependent upon properties of the flow near walls. y^+ values are extracted as part of post-processing from a CFD solver.

$$y^+ = \frac{u^* y}{v} = \sqrt{\frac{\tau_w}{\rho}}$$

Equation 4. Calculating y+ values

Where; y^+ = dimensionless distance from a wall to the first node in a mesh, y = distance from a wall to the first node in a mesh (m), v = kinematic viscosity of a fluid (m^2/s), ρ = density of fluid (kg/m^3) and τ_w = wall shear stress (kg/ms^2).

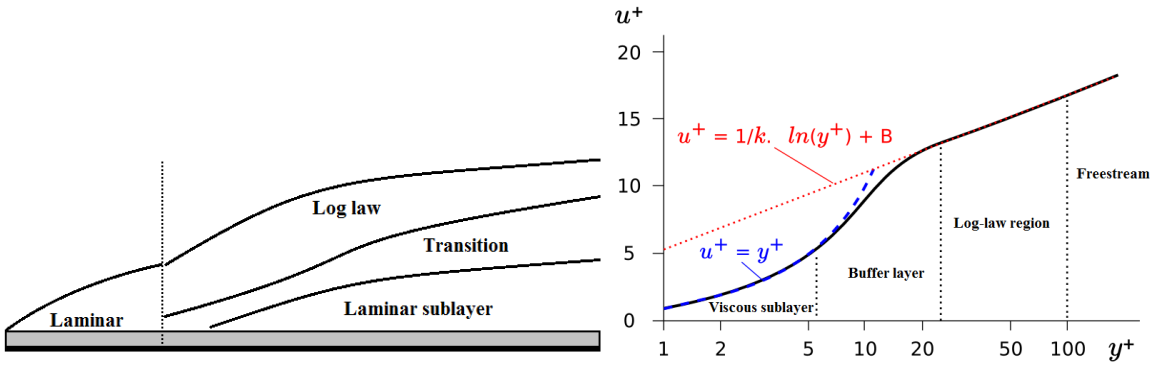

Figure 6. General form of boundary layer over a flat plate (left) and wall velocity profile for wall functions (red) and resolving the flow (blue) [29]

To resolve or model flow near walls, generally a boundary layer mesh is used (Figure 7). This is a set of layered hexahedral cells next to a wall. They reduce the number of cells used in wall-normal directions, and provide a consistent y^+ value across the wall for wall functions (wall modelling).

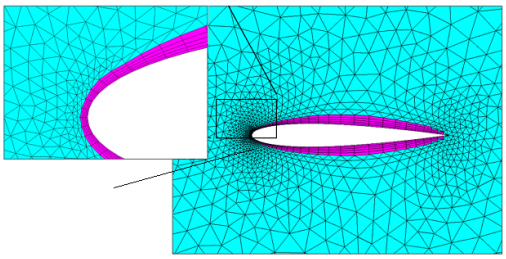

Figure 7. Boundary layer hex cells (purple), tetrahedral cells (cyan) [30]

3.2. Topographical Data Conversion

Lidar data at a 2m vertical and 1m horizontal resolution was obtained from the Environment Agency Geomatics group. The data came in two formats; a digital surface model (DSM), which includes all surface features including vegetation and buildings, and a digital terrain model (DEM), which includes only the bare topographical features. Ideally, the choice would have been to use the DSM surface for generating STL files. However, there were issues with the data files. DSM files included features of the Humber Bridge itself, shown as a blockage in the flow (Figure 8). There were also holes and defects in these STL files in areas of water caused by Lidar being unable to accurately pick up the moving surface of bodies of water. The OpenFOAM SHM utility does not work if the STL surface specified is not fully solid. To compound this issue, STL files are problematic to edit. As a compromise, DEM files were used to create the STL files required for meshing in OpenFOAM, with a slight reduction in the resolution and number of surface features.

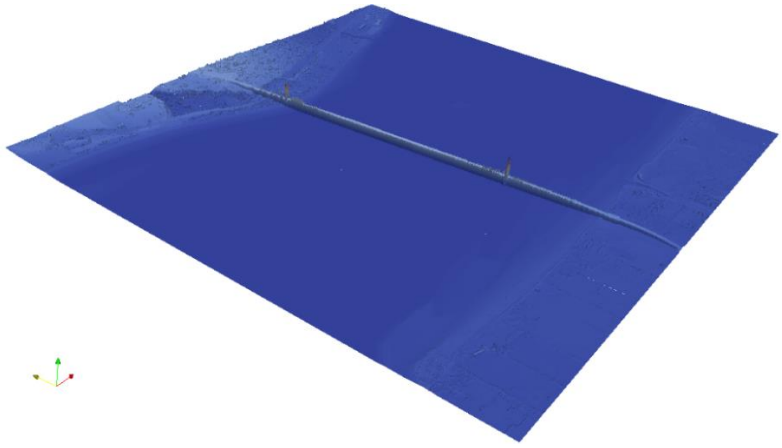

Figure 8. DSM of Humber Bridge terrain extracted from Lidar data

Lidar data is provided in 1km × 1km squares in Arc ASCII text files (.asc). There were several options in conversion to STL data files. For $1km^2$ grids, the terrain software GlobalMapper was useful, as it can batch convert native file types to STL. This software was obtained from the Penryn campus of Exeter University. Usually, there is a licence cost of £275 for this software. An alternative method is suggested, when several grid squares (terrain greater than $1km^2$) were required for wind flow analysis. The method first converted the Arc format to a matrix of XYZ points using a MatLab script, obtained online [31]. The XYZ points from a $9km^2$ area were combined. At this point there were two options to pursue. Matlab and an STL writing script (stlwrite.m) could have been used. This was the methodology used by Holdaway et al. in assessing the feasibility of using OpenFOAM to simulate the ABL [32]. It was found that MatLab could not handle large XYZ datasets for the area to be studied. An alternative solution was found using MeshLab. This surface meshing software was used to import XYZ data. Two filters were used to create an STL surface; normals, curvature and orientation, to compute normals for the XYZ point set, and a remeshing, simplification and poisson surface reconstruction. The STL files created by this method were exported in ASCII text format to OpenFOAM for meshing and CFD analysis.

3.2.1. SnappyHexMesh

SHM is the OpenFOAM native mesher. It builds from a prerequisite hexahedral mesh, created using the *blockMesh* utility. To snap to an STL surface, the initial mesh has to fully encompass it. OpenFOAM works in a standard co-ordinate system. The convention adopted in this project was, *x*, in the direction of flow, *z*, as height, and *y* as depth. The STL terrain surfaces produced were of full scale and with global coordinates. To produce a domain with this complex terrain, the initial blockmesh had to be translated in space to the same global position as the STL

surface. This was achieved using the utility *transformPoints –translate* and looking up the first and last XYZ coordinates in the STL file. SHM operates in 3 stages; castellation, snapping to the STL surface, and the addition of a boundary layer mesh through expansion of cells closest to the walls. The *locationInMesh* section of the SHM setting was used, to specify that the mesh be above the surface of the terrain. While it is a robust meshing tool, SHM has a poor record of adding boundary layer cells. Despite a large amount of effort, research and investigation, adding layers to complex terrain proved to be a futile exercise. There was an inverse relationship between the number of successfully added boundary layer cells and the resolution of the terrain surface. Alternative OpenFOAM meshing tools have been used (refer to section 2.2.2), but these were not implemented in this project.

3.3. CFD Simulations

From the literature studied in regards to the ABL, flow over complex terrain and computational resources available, it was determined to use the k-epsilon turbulence model. Given the accuracy of results given by the k-epsilon turbulence model in modelling flow over the Askervein hill, this model was a good compromise between numerical accuracy and computational expense. There was also incentive to provide a mean flow profile derived from flow over terrain to the CFD subgroup for implementation into a final DES case of flow over the Humber Bridge deck. In contrast to literature studies of simulated wind flow over the Askervein hill, it was decided to use the time marching solver, PISO, in comparison to the steady state solver, SIMPLE. This was used because flow over terrain is inherently unsteady and complex surface features can induce transient flow instabilities that may not allow convergence with a steady state solver [33]. A steady solver also only gives one instantaneous solution of a transient flow. With the choice of a transient solver, it is correct practice to keep the Courant number (C_o) below a maximum value of 1 (and ideally 0.2) to satisfy the Courant-Freidrichs-Lewy condition (Equation 5). This number is a definition for the number of cells a simulated fluid particle travels through in one time step. LES and DES simulations have stricter constraints, and a maximum C_o of 0.5 is required for stability.

$$\frac{U_{ref}\Delta t}{\Delta x} \leq Co_{max} = 0.5$$

Equation 5. Courant-Freidrichs-Lewy condition.

Where, U_{ref} = freestream or maximum velocity, Δt = time step and $\Delta x \approx$ domain length$_x$ /number of cells in x direction.

3.3.1. Boundary Conditions

Appropriate boundary conditions were set in accordance with the '*Best practice guideline for the CFD simulation of flows in the urban environment*' [34], and recommendations by Blocken et al. [35] for simulating the ABL; a sufficiently high resolution mesh near to the ground, obtaining a horizontally homogeneous solution (a flow profile not varying in the horizontal plane), y^+ values greater than the physical roughness (Ks) of the terrain and a clear relationship between physical roughness, Ks, and aerodynamic roughness, z_0. Without these considerations, results for flow of the ABL over complex terrain will have some level of error. Blocken et al. state that it is not currently possible to achieve all these conditions together. This is because a very high resolution at the ground conflicts with the minimum y^+ value of 11.6 for RANS turbulence models and violates the roughness (Ks) constraint.

Holdaway et al. [32] summarised approaches to obtain an accurate solution of the ABL. These included; adapting the inlet for realistic flow profiles matching wind tunnel/experimental data, adapting roughness for the terrain, and changing the top boundary patch to ensure the flow suits the enclosure. Approaches by Richards & Hoxey [16], Yang et al. [36] and O'Sullivan et al. [37] were compared. A conclusion was reached that Yang et al. and O'Sullivan et al. had the most accurate top patch boundary conditions. However, this was only proven for flat terrain. The Yang et al. approach requires experimental data to fit their equation, making their work unusable in the context of this report (where no experimental data exists). In a recent thesis of flow over complex terrain [38], O'Sullivan showed that a constant shear stress should be applied across the top patch of the domain, with appropriate values for k and ε. Previous studies stated that a slip condition is acceptable for the top and side patches, as long as the top patch sufficiently high above the terrain. Slip conditions have no effect on a fluid velocity in planes parallel and close to them, making them acceptable for the side patches. O'Sullivan demonstrated that while the formation of stream wise gradients are reduced by increasing the height of the top patch above the terrain, that velocity and TKE errors occur in the flow. Increasing the height of the domain sufficiently to minimise errors invalidates the assumption of not including the Coriolis effect on the flow so the shear stress condition is required.

The following approach was taken in setting boundary conditions for all simulations; a user defined groovyBC inlet profile using the OpenFOAM swak4Foam library, a zero gradient pressure outlet, slip conditions for the side patches and a constant shear stress for the top patch. The shear stress condition was applied using the *fixedShearStress* patch type. A roughness wall

function, *nutkRoughWallFunction*, was used for the terrain patch generated from the STL surfaces (see section 3.2). In all cases, dry air properties were used; ν=1.51×10^{-5}m^2/s and ρ=1.2kg/m^3 and flow was assumed to be incompressible.

3.3.2. Surface Roughness and K-epsilon Parameters

Values for k and ε were calculated using the method of Richards & Hoxey (Equation 6). Calculating these correctly ensured that the inlet velocity, turbulent profiles, and shear stresses, were in equilibrium. The top patch boundary condition was defined with a constant shear stress, using the method of O'Sullivan (Equation 7).

$$u_* = \frac{u_{ref}\kappa}{\ln\left(\frac{z+z_0}{z_0}\right)} \qquad k(z) = \frac{u_*^2}{\sqrt{C_\mu}} \qquad \varepsilon(z) = \frac{u_*^3}{\kappa(z+z_0)}$$

Equation 6. Calculating k and epsilon

$$\frac{\partial u}{\partial z} = \frac{u_*}{\kappa(z+z_0)} \qquad \frac{\partial k}{\partial z} = 0 \qquad \frac{\partial \varepsilon}{\partial z} = \frac{-u_*^3}{\kappa(z+z_0)^2}$$

Equation 7. Top patch shear stress boundary condition

Where; u_{ref} = mean wind velocity at height z, z_0 = surface roughness length, κ = 0.41 (von Karman's constant) and u_* = atmospheric boundary layer friction velocity.

Surface roughness lengths were set in OpenFOAM through Ks (sand grain roughness), and Cs (roughness constant). These were calculated from standard roughness lengths [39], although there is inconsistency in the relationship between the values of this method. Typically, Ks = 30×z_0. As suggested in the work of Stangroom [40], Ks = 7.5×z_0, gives more suitable values.

3.4. Askervein Hill Validation Case

A case of flow over the Askervein hill was set up. This was to validate a set of initial conditions to use in future cases of wind flow over the terrain near the Humber Bridge. This allowed for a comparison of numerical results to those from literature [14,18,19], and ascertain the likely error in future results. OpenFOAM ABL inlet conditions were used; *atmBoundaryLayerInletVelocity* and *atmBoundaryLayerInletEpsilon*. Using *#include* in initial conditions, parameters from literature were implemented (Table 1). These initial conditions calculate a log law inlet profile for wind, *U(z)* (Equation 8) and turbulent quantities (Equation 6). Due to the complex terrain contours of the hill, the computational mesh included some non-orthogonal cells (Figure 10). Appropriate corrections were applied in the solution algorithm by

including a number of non-orthogonal corrector loops. All simulations were run in parallel to reduce computation time using the OpenFOAM utility, *decomposePar*, and the Unix *mpirun* function.

$$U(z) = \frac{0.6692}{\kappa} \times \ln\left(\frac{z}{0.047}\right)$$

Equation 8. Log law profile, Eurocode 1 (EN-1991-1-4:2005 Wind actions).

Table 1. Askervein Hill case parameters

Parameter	**Value**
Freestream velocity (U_{ref})	*8.9m/s*
ABL friction velocity (U^*)	*0.63m/s*
Roughness height (z_0)	*0.03*
Height of freestream velocity (z)	*10m*
Sand roughness value (Ks), Roughness constant (Cs)	*0.225, 0.5*
Domain dimensions (x,y,z)	*(2600m,2500m,485m)*
Turbulent kinetic energy, TKE (k)	*2.29m^2/s^2*
Turbulent dissipation rate (ε)	*0.06m^2/s^3*
Mesh size	*1,674,951 cells*
Divergence schemes	*Upwind, linear and limitedLinear 1*
Solution control, Turbulence model.	*SIMPLE – k-epsilon. Convergence: 1×10^{-5} for k, ε. 1×10^{-6} for U, p*

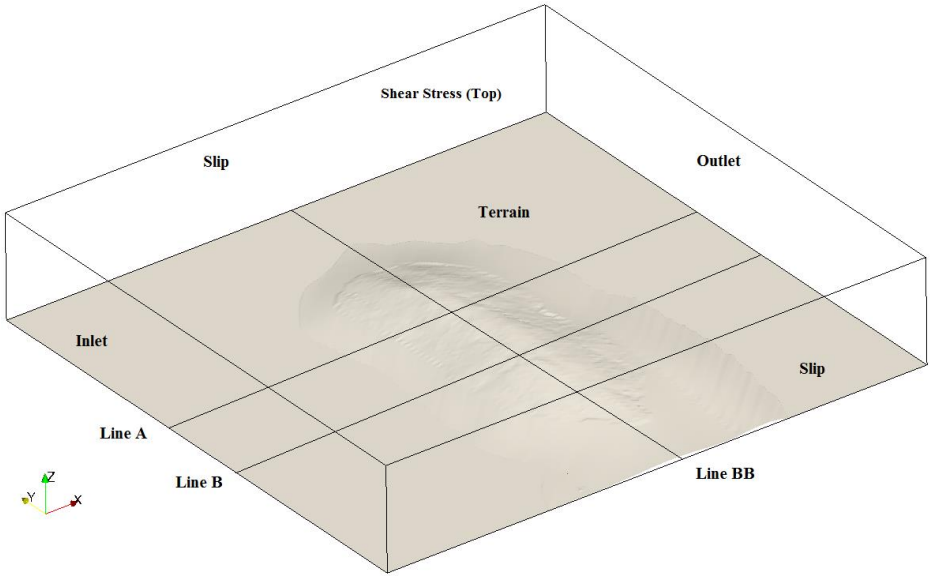

Figure 9. Askervein Hill STL with domain boundary conditions and experimental recording stations (lines: A,B,BB)

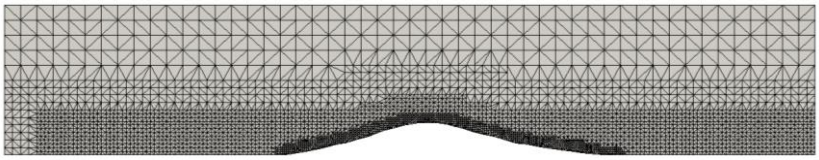

Figure 10. Mesh refinement over hill

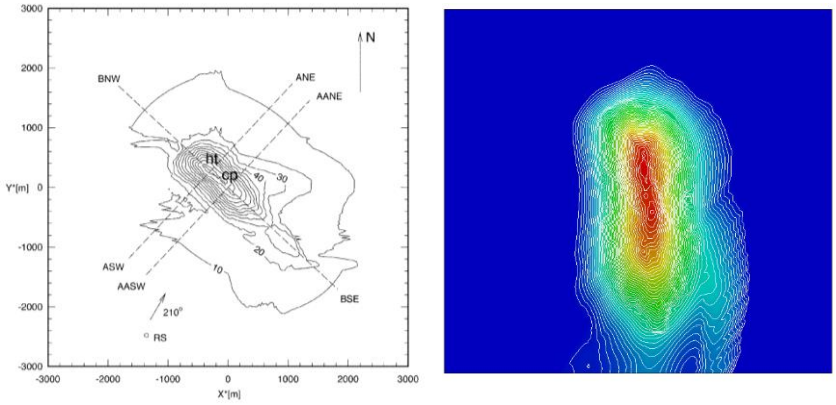

Figure 11. Askervein Hill topographic map [18] (left) and elevation contours (right)

3.5. Humber Bridge Terrain

With the Askervein test case validated, a study was made of crosswind wind flow over terrain near the Humber Bridge. Initially, a full case was attempted with both a bridge deck and complex terrain. Achieving a mesh of sufficient quality and of a practical number of cells was problematic. This was due to the requirement to mesh the terrain at a 1m resolution to capture local features and include the entire span of the bridge deck (2100m long). Poor resolution of the mesh around the bridge deck meant that accurate and stable numerical simulation was hard to achieve. To overcome these problems a different method to determine the effect of terrain on the bridge deck was used. The effect of terrain on the flow was implicitly derived through observing the change in velocity profiles across the domain (section 3.6). This was also further explored as part of CFD subgroup DES simulations.

A mean wind profile for the area was obtained from a MET office UK wind map. This map was generated from 2,500 monthly and annual average wind speeds over a 30 year period. It has been well verified against observational data and is a good alternative to collecting experimental wind readings (a costly and lengthy task). An average difference between the database and observed wind speed has been calculated as ±0.4m/s [41]. A groovyBC inlet profile taken from the wind map data for the local area was implemented:

```
variables           "z=pos().z;";
```

```
valueExpression     "vector(((z<10)?5:(z<25)?(5+0.053*(z-10)):(z<45)?5.8+(0.03*(z-
                    25)):6.4),0,0)";
```

Initially the case was run with a domain height of 200m. It was determined that the velocity profile remained constant, once a height of 60m had been reached. The domain was reduced in height in the z direction to reduce the overall cell count and to improve resolution at the ground. An average roughness height was set for the domain, based upon ~70% of the surface being water (z_0 = 0.005) and ~30% being shrubbery and small buildings (z_0 = 0.25) [39]. For fully developed flow, the case was run for 1600s of simulated time. This meant that the slowest velocity within the flow would pass through the domain 2.5 times ($\frac{2900m}{4.5m/s} \times 2.5 \approx 1600s$).

Table 2. Terrain case parameters

Parameter	**Value**
Inlet velocity (U_{ref})	*6.4m/s (groovyBC)*
ABL friction velocity (U^*)	*0.63m/s*
Roughness height (z_0)	*0.076*
Height of freestream velocity (z)	*75m*
Sand roughness value (Ks), Roughness constant (Cs)	*0.59, 0.5*
Domain dimensions (x,y,z)	*(2900m,2900m,75m)*
Turbulent kinetic energy, TKE (k)	*0.745m^2/s^2*
Turbulent dissipation rate (ε)	*0.0025m^2/s^3*
Mesh size	*1,023,987 cells*
Divergence schemes	*Upwind, linear and limitedLinear 1*
Solution control, Turbulence model, Time step (Δt)	*PISO, k-epsilon, 0.1s (adjustable time step for max. Co=0.2)*

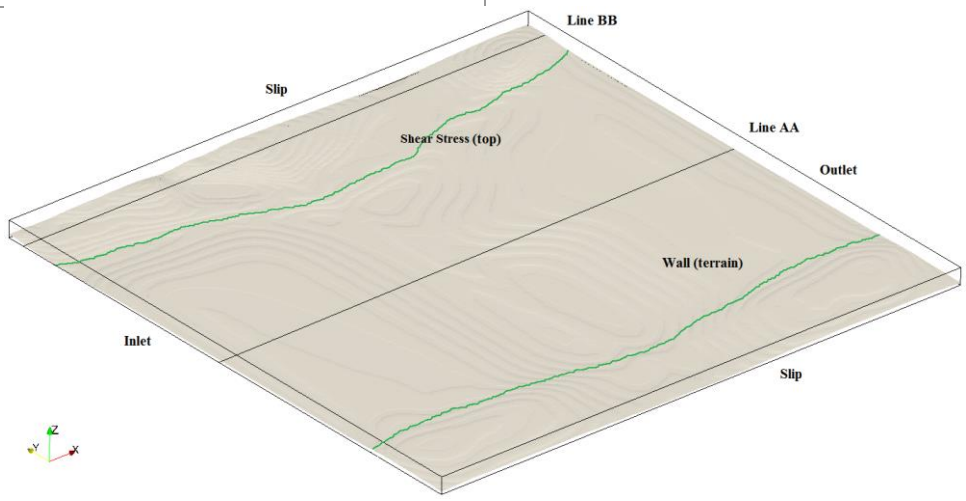

Figure 12. Flow domain for Humber Bridge terrain (green defining the river bank). STL surface produced from MeshLab.

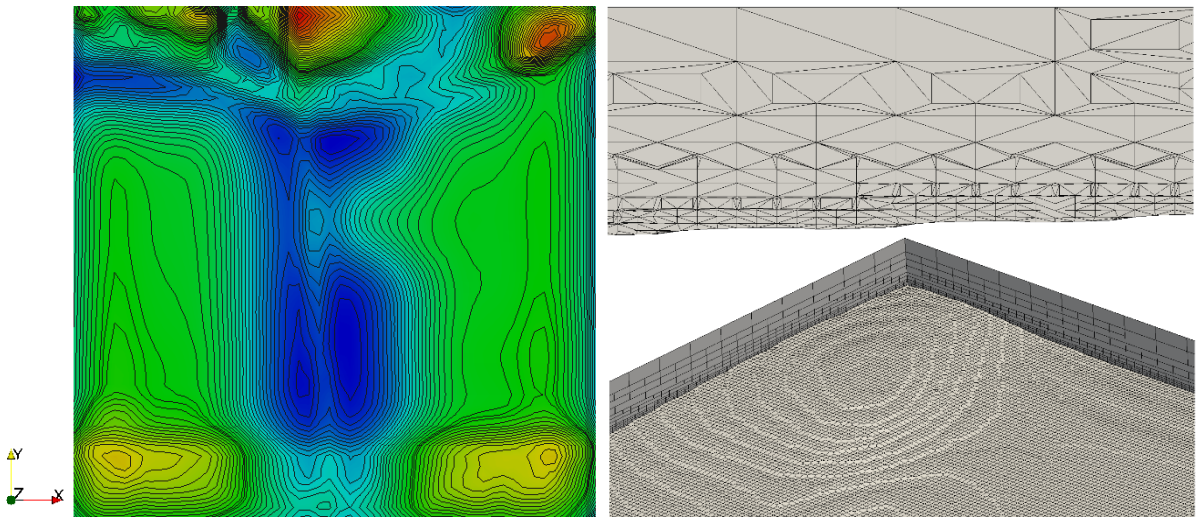

Figure 13. Elevation contour for terrain, red=high, blue=low (left). Close-up and section view of meshed terrain (right)

3.6. Effect of Flow upon Bridge Deck

Wind profiles were obtained from the terrain study. To determine the effect changes in wind flow would have on the Humber Bridge deck two flow cases were set up. The first had the same inlet condition specified for the Humber terrain case. The second case used a flow profile calculated from the Humber terrain case. This profile was produced by curve fitting to a polynomial format (Figure 19). The chosen terrain was at its most complex along the line BB (Figure 12). The data from line AA was largely dismissed, because the elevation was not representative of the flat surface of the water, but the surface of the river bed (Figure 13). The velocity profile of the wind flow over the terrain was taken just before the site of the bridge (~1400m along the domain in the x direction). The groovyBC inlet profile was as follows:

```
variables    "A=7e-9;B=-1e-6;C=1e-4;D=-0.0038;E=0.0769;F=-0.826;G=-2.9666;
zPos=pos().z;";

valueExpression    "vector(((A*pow(zPos,6))+(B*pow(zPos,5))+(C*pow(zPos,4))+
(D*pow(zPos,3))+(E*pow(zPos,2))+(F*zPos)+(G)),0,0)";
```

Only a solid bridge deck was modelled to reduce meshing complexity. The same mesh was used for both inlet types (Figure 14). The k-omegaSST turbulence model was used for transient flow over the deck as it is a good model for external aerodynamics. Parameters for the k-omegaSST model were calculated from Equation 3 using the bridge deck as the characteristic length (Table 3). Coefficients of lift and drag on the bridge deck were calculated using the length of the deck and the frontal area (4.5m×8m). The simulation was run for 100s to pass flow through the domain 3 times, ensuring fully developed flow ($\frac{120m}{4.5m/s} \times 3 \approx 80s$).

Table 3. Bridge deck simulation parameters

Parameter	**Case 1 (Standard Inlet)**	**Case 2 (Terrain Inlet)**
Inlet velocity (U_{ref})	*6.4m/s (groovyBC)*	*7m/s (groovyBC)*
Domain dimensions (x,y,z)	*(120m,8m,60m)*	*(120m,8m,60m)*
Turbulence model	*k-omegaSST*	*k-omegaSST*
Turbulent kinetic energy, TKE (k)	*0.027 m^2/s^2*	*0.183m^2/s^2*
Specific turbulent dissipation rate (ω)	*0.076m^2/s^3*	*0.035m^2/s^3*
Mesh size	*676,256 cells*	*676,256 cells*
Divergence schemes	*Linear and limitedLinear 1*	*Linear and limitedLinear 1*
Solution control, Turbulence model	*PISO – k-omegaSST*	*PISO – k-omegaSST*
Time step (Δt)	*0.001s (adjustable time step, max. Co=0.2)*	*0.001s (adjustable time step, max. Co=0.2)*

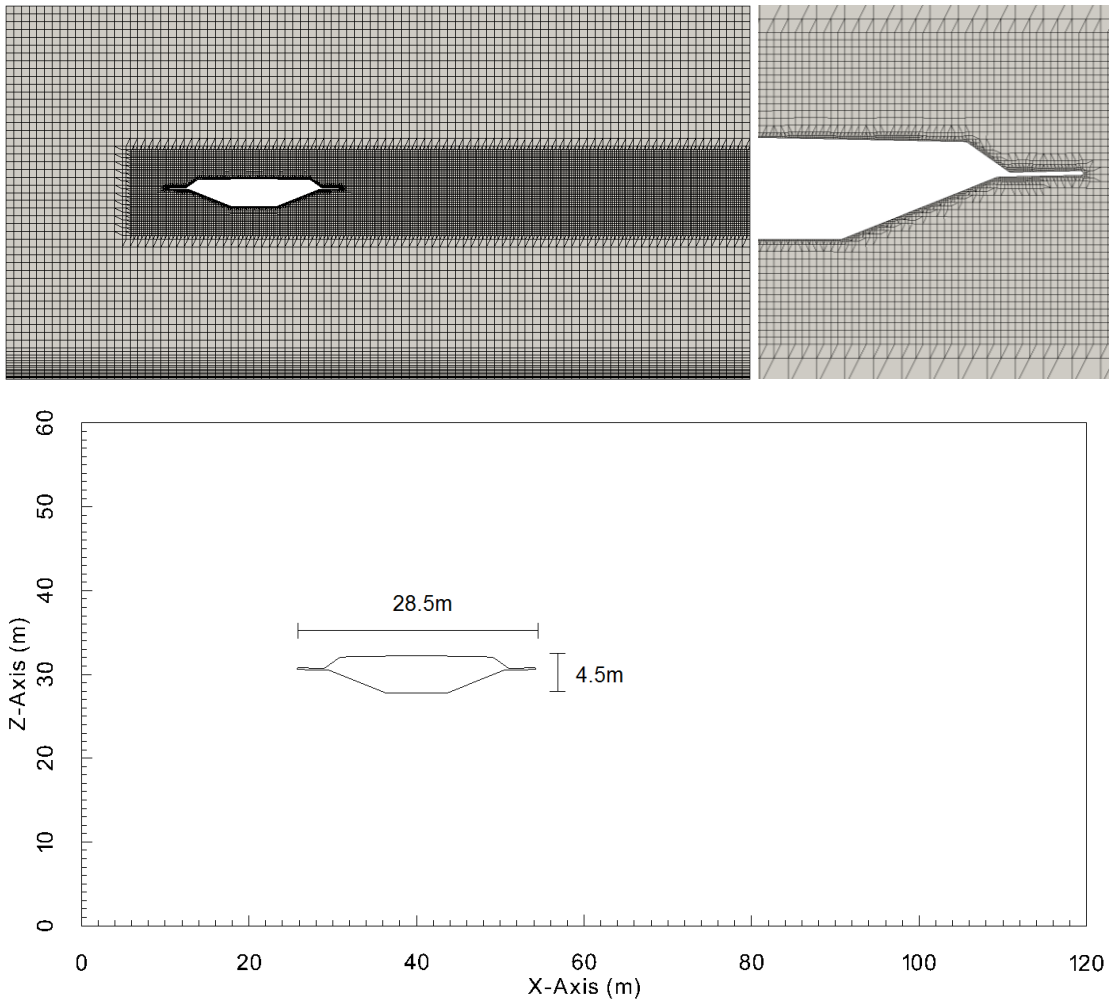

Figure 14. Mesh and domain for bridge deck

4. Computational Results and Discussion

4.1. Askervein Hill Results

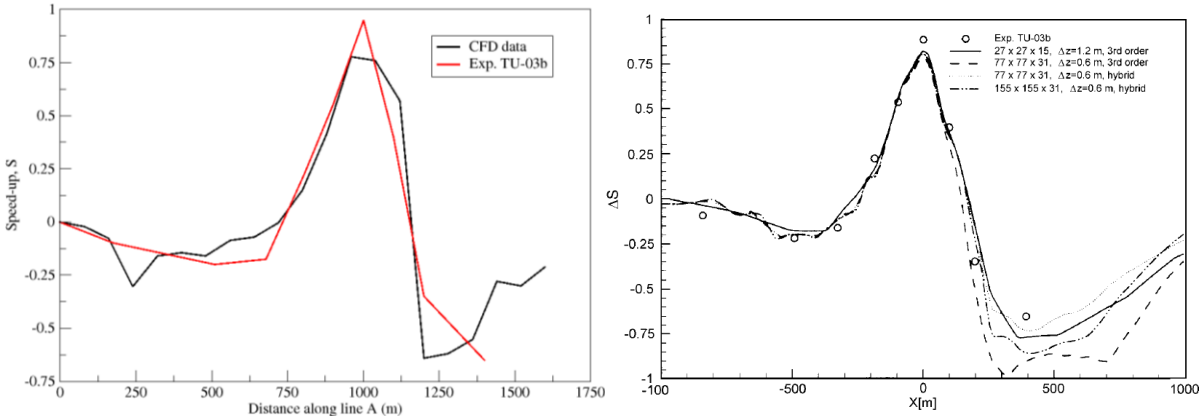

Figure 15. Speed-up comparison of experimental data (right) to CFD (left) across line A

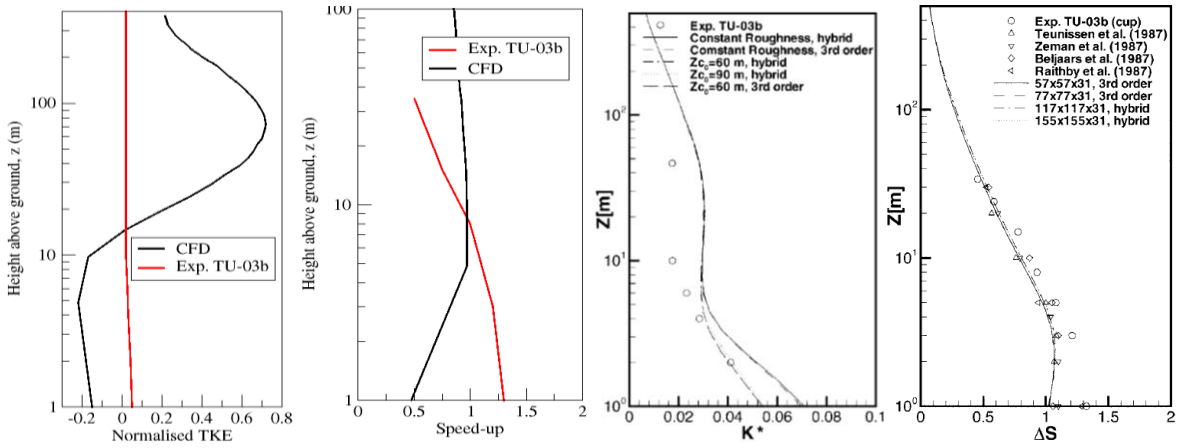

Figure 16. Normalised TKE and speed-up comparison of experimental data (right) to CFD (left) at top of hill

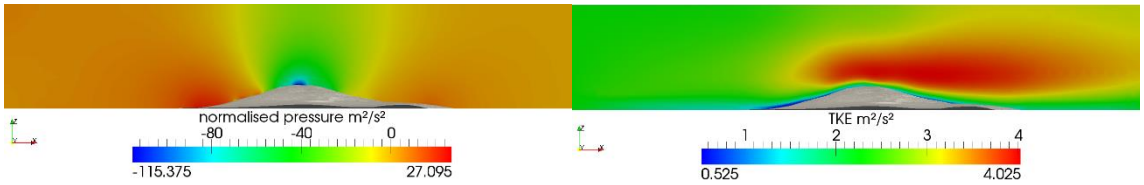

Figure 17. Pressure contours (left) and TKE contours (right) over Askervein Hill

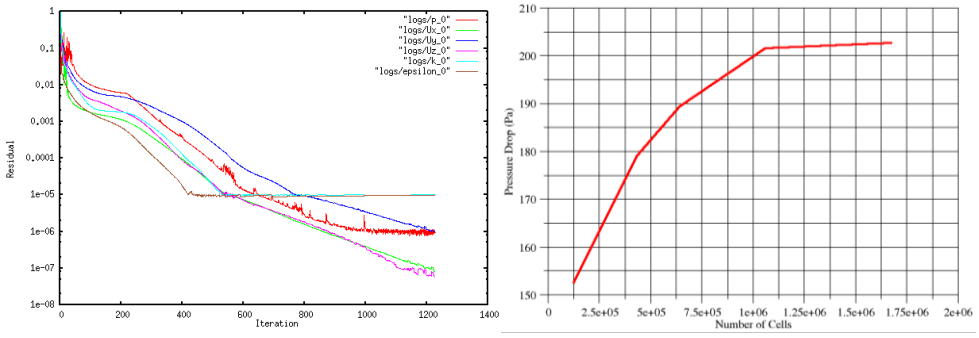

Figure 18. Residuals Vs Iteration for convergence (left). Mesh convergence study for pressure drop (right).

4.1.1. Analysis and Discussion

For conciseness results were only sampled and compared with experimental data along line A. Velocity speed-up over the hill was calculated to determine the effect the hill had on the flow (Equation 9). TKE values were also normalised where, U = velocity, U_{ref} = reference inlet velocity, TKE = TKE and TKE_{ref} = reference inlet TKE.

$$Velocity\ speed-up, S = \frac{U-U_{ref}}{U_{ref}} \qquad Normalised\ TKE = \frac{TKE-TKE_{ref}}{TKE_{ref}}$$

Equation 9. Calculating non-dimensional speed-up and normalised TKE over terrain

Data was extracted along line A at a height above the ground of 10m. The velocity speed-up compared well to the numerical results of Castro et al., with a minimum percentage error of 9.7%. When compared to the experimental results of Taylor & Teunissen, a maximum percentage error of 82.9% was present, particularly in the leeward side of the hill. At the top of the hill, where speed-up was highest, the percentage error was smaller, from 35-20% different to the experimental results. These large errors are partly attributable to using the SIMPLE algorithm, because the steady state formulation imposes constraints on transient aspects of the flow. Some transient physics within the flow can be seen, where the residuals of pressure and velocity fluctuate near convergence (Figure 18). No relaxation was used in the simulation, and accuracy was traded off with a relatively fast convergence in 1241 iterations. Errors in speed-up may be attributable to other factors. The plane that results were sampled from in the CFD simulation may not have been along the same line as the experimental data. This is because no co-ordinates were given in literature that precisely defined line A (the location of the experimental data stations). Another cause of errors may be the size of the domain; if the co-ordinates in the x-direction were not matched correctly to the experimental data, then again, CFD data may have been sampled at different points along the x-axis. A lack of co-ordinates for the recording stations hampered the ability to accurately reproduce the results of the study using CFD. Contributing to errors is the comparison with experimental data. Linear speed-up is assumed between the 9 discrete wind recording stations, which may not be representative of the flow between them. Differences in results to those of Castro et al. are partially attributable to their use of more accurate 3rd order differencing schemes and a different computational mesh. 1st order upwind differencing was used in this case until a stable solution was achieved, with central differencing applied in later iterations to improve the accuracy of results.

As seen in Figure 18, mesh independent results were not achieved, and a smaller than expected flow separation observed in the leeward side of the hill. This problem was also found to be the case by Castro et al. and is a feature of the k-epsilon model in studies of flow over the Askervein Hill. For this reason, in future studies of the Humber Bridge terrain, a sensibly high mesh resolution was used, while taking into account the length of time taken to run the case with the transient solver, PISO. As expected from this case the speed-up followed the lye of the land.

Figure 16 shows the velocity and TKE Z-profiles values at the top of the hill at line A. The normalised TKE profile shows almost no correlation to those from the experimental data, with a peak at a height of 80m (Figure 17). The speed-up at the top of the hill also shows inconsistencies with the experimental results. The large discrepancies in these values may be attributed to an incorrectly evaluated terrain roughness and the cell centre of the terrain-adjacent cell being above the log-law region of the boundary layer. These graphs indicate that wall modelling occurs up to a height of 5m above ground (the height of the first cell). Differences in the height of wall modelled flow is one reason for differences in results because the terrain-adjacent cell height for the study by Castro was 0.5m. This is consistent with the calculated minimum $y+$ value of 4300, which ideally should be between 30 and 300 to accurately model the terrain boundary layer. As discussed in section 3.2.1, creating a boundary layer mesh to negate this issue using the OpenFOAM mesher, *snappyHexMesh*, was problematic. Had different meshing software been used, this obstacle may have been overcome. Castro et al. also implemented a variable surface roughness, with a reduced roughness length over the peak of the hill. Importantly, the roughness parameters are used to define the k and ε values for the ABL and so could account for the large differences between the experimental and numerical results.

Qualitatively speaking, a sufficiently complex terrain such as the Askervein Hill should include time dependent flow features. Based upon this simulation, and the results of Castro et al., there is a strong argument to model flow over terrain with a time marching solver in order to capture intermittent transient flow components. This study also demonstrated that flow over terrain using the k-epsilon model is very sensitive to initial conditions, which are based upon several parameters such as surface roughness. This parameter is difficult to set correctly. Only by setting these values correctly, can RANS models accurately simulate ABL and flow over terrain accurately. Given the errors present in this study, it was likely that future studies using a time marching solver, would have slightly smaller errors, in the range of 10-30%. Errors may

be reduced further by refining the mesh near the terrain, to reduce $y+$ values to a reasonable level.

4.2. Humber Bridge Results

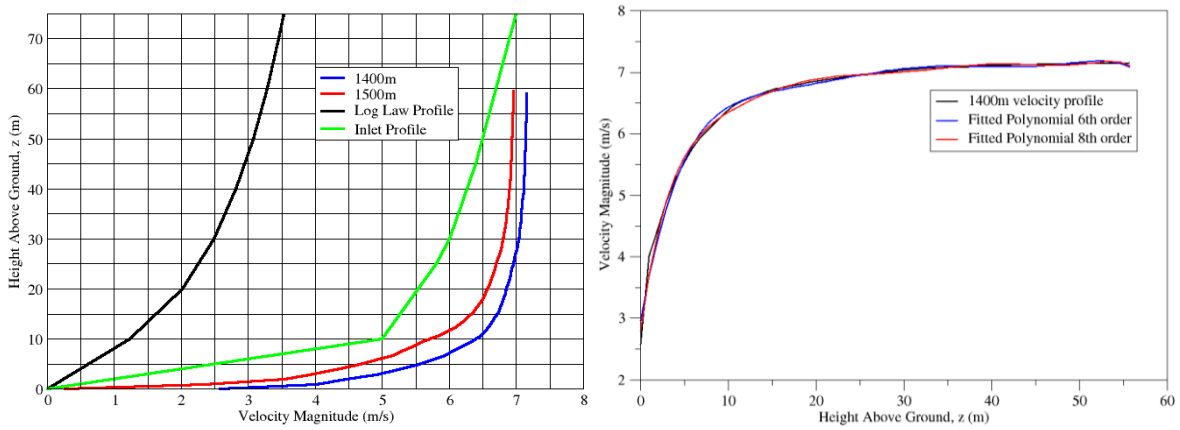

Figure 19. Velocity profile comparison across terrain (left) and polynomial approximation to 1400m velocity flow profile

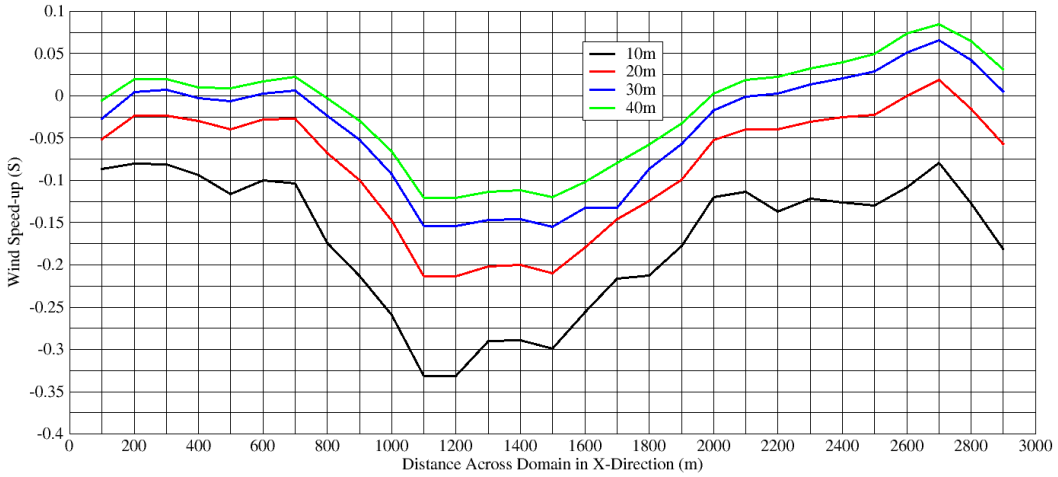

Figure 20. Speed-up along line AA

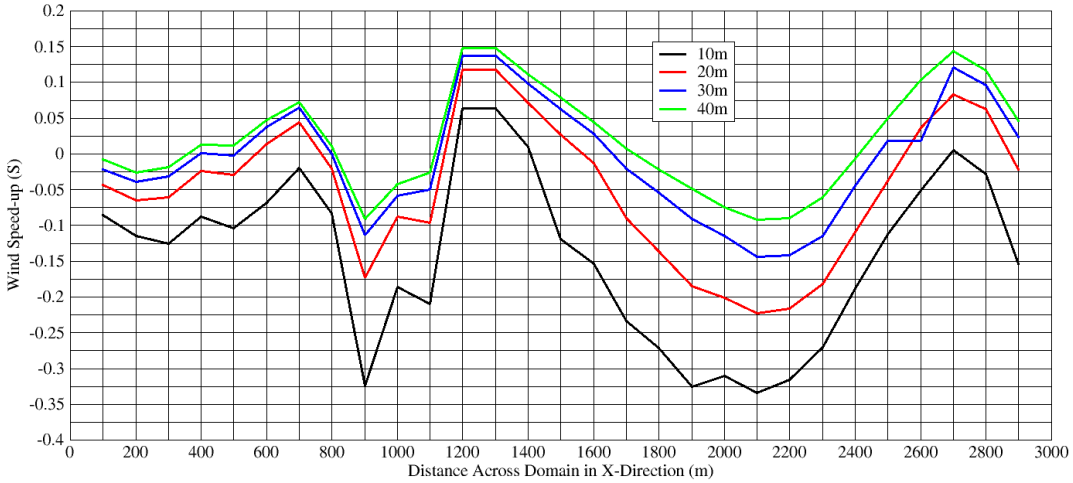

Figure 21. Speedup along line BB

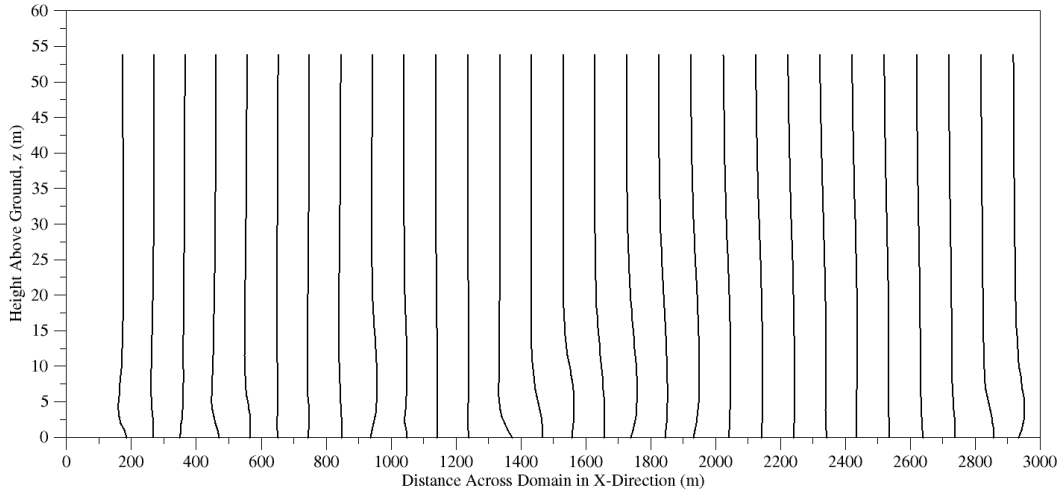

Figure 22. TKE profiles across terrain at line BB

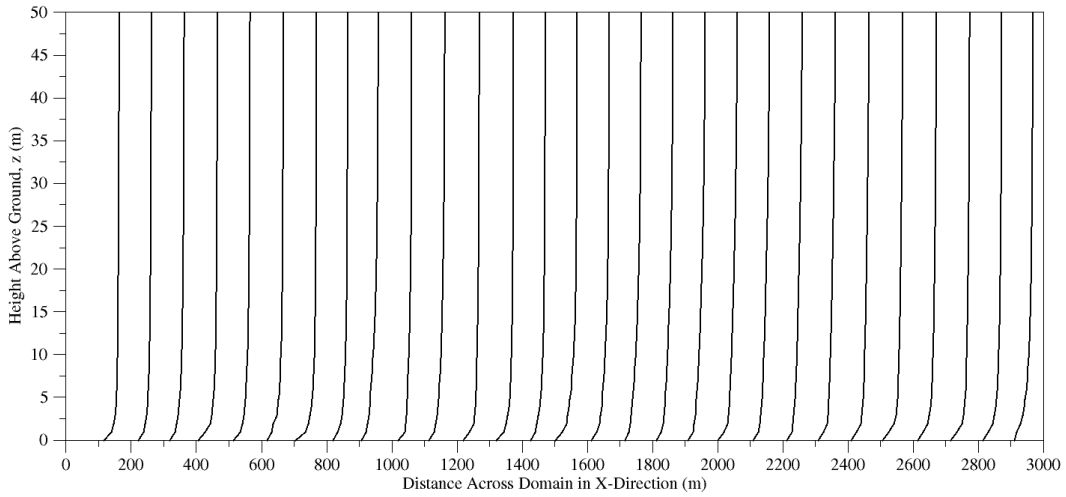

Figure 23. Velocity profiles across terrain at line BB

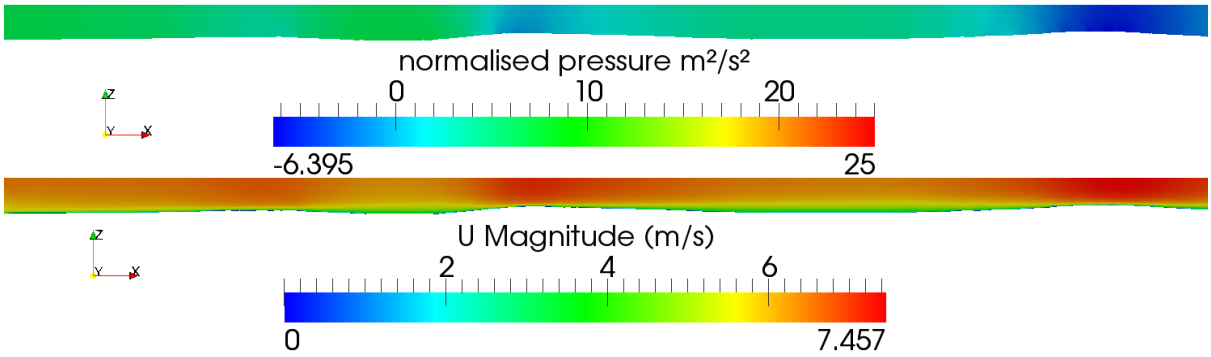

Figure 24. Contours of pressure and velocity across the domain at line BB

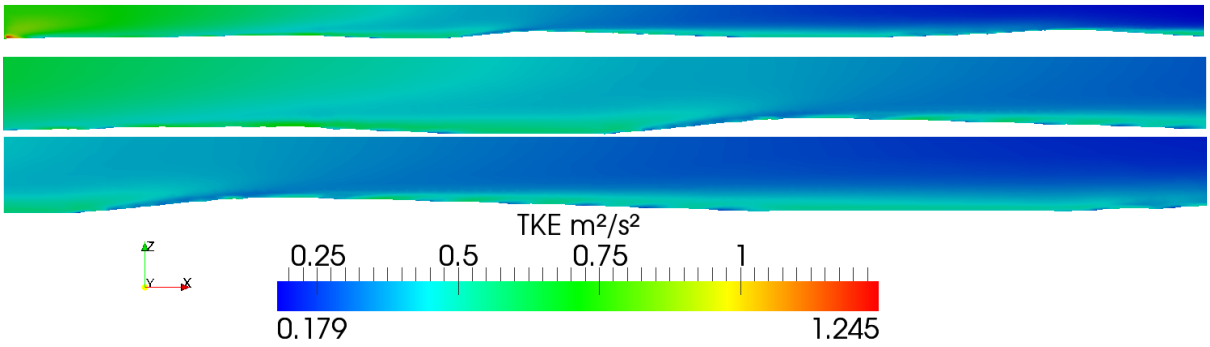

Figure 25. Contours of TKE across domain (top) and close-up (bottom)

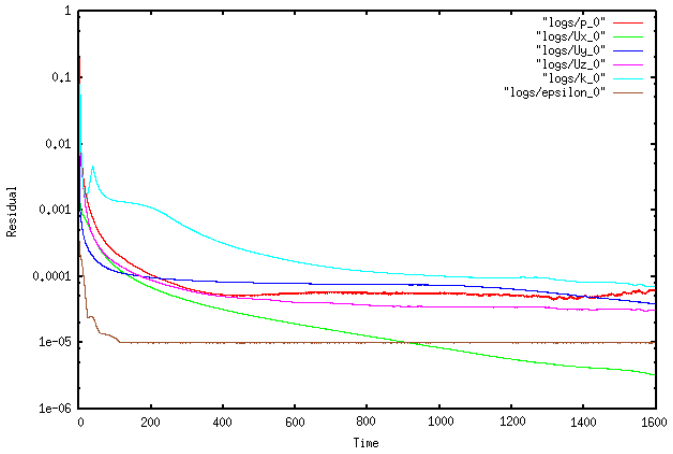

Figure 26. Residuals over time

4.2.1. Analysis and Discussion

Data from this study was sampled from the CFD simulation along line BB. The data along line AA is invalidated by the fact that the generated mesh is not representative of the surface water of the Humber Estuary, but instead the bed of the Estuary. As a flat body of water with a very low surface roughness, it is unlikely to develop especially turbulent wind profiles, with little wind speed-up. Data was sampled along line BB, as the topography includes interesting features that may have an effect on wind flow and therefore the Humber Bridge deck.

The inlet profile for this simulation was taken from the MET office wind map (Figure 19). Using the wind map inlet was a more accurate representation of the flow in this area compared to the standard log law inlet profile used in industry. The changes to the TKE and velocity of the flow can be seen to correlate with changes in height of the topography (Figure 24). As the profiles for TKE and velocity develop along the domain, they reach near constant values above the ground at heights of 35-40m (Figure 23). This is important because the Humber Bridge deck in this terrain is 30m above the ground at its highest point. With changing profiles encompassing the bridge deck, it is possible for changes to the wind flow (due to topography),

to have a resulting effect upon the deck. This was quantified in a later case study (section 4.3). The velocity profile of flow over the most complex component of the terrain (along line BB) was extracted. The profile was taken at a point 1400m along the domain, the location of the Humber Bridge. The profile was approximated with the 6th order polynomial; $y=-7\times10^{9}x^{6}+1\times10^{6}x^{5}-1\times10^{4}x^{4}+0.0038x^{3}-0.0769x^{2}+0.826x+2.9666$ (Figure 19). This velocity profile was supplied to Richmond [2] for use as an ABL-derived mean inlet profile for DES CFD subgroup case studies of flow over the Humber Bridge deck. As a mean profile was required for the CFD subgroup simulations, it validates the choice of using RANS models for terrain flow. If the fluctuating nature of flow over terrain had been required, DES could have been used as the solver. This was not undertaken for these reasons, as well as the high computational expense involved in such a simulation.

Figure 21 shows how the wind velocity changed over the features of the terrain. Data was sampled at heights of 10, 20, 30 and 40m. In the case of this terrain, the wind velocity slowed down between hills by a greater factor (up to S=-0.325) than it did in speeding up (S=0.15). There were three peaks and troughs of speed-up, consistent with the layout of three minor topographical features. This is consistent with the separation seen over these features in contours of velocity and pressure (Figure 24).

Without wind tunnel data or field measurements, the accuracy of these results in representing real world wind flow over terrain cannot be ascertained. In reference to the Askervein Hill study, similar boundary conditions were used, and the PISO solver likely gave improved results than would have been obtained with a steady-state formulation. Enough flow was simulated (1600s) for the flow to pass through the domain several times and reach a dynamic steady-state. This was observed in post processing, where magnitudes for velocity and pressure reached constant values. Some trust has to be placed in the shear stress top boundary condition suggested by O'Sullivan, as well as the choice of initial conditions, using the method of Richards & Hoxey. Given the TKE results of the Askervein Hill study, and the tendency of the k-epsilon model to over predict TKE of the flow, it is possible that flow separation and wind speed-up may be over-predicted in this study. While the k-epsilon model was suitable in this instance, in canyon flow or strongly rotational flow, other two equation models (e.g. RNGk-epsilon, realizable k-epsilon) may be required in order to accurately model turbulence with good stability. It still falls to the user to critically approach flow over terrain and choose an appropriate RANS turbulence model for rotational or separated flows.

Quantifying the potential errors in the results was not practically possible without experimental data, although sources of error may be identified; one such source is near the inlet of the domain (Figure 25). TKE is very high at the point where flow enters the domain and impinges upon a small topographical feature. This may reduce the accuracy of results through the introduction of excessive turbulence at such an early point in the domain. If the study were to be repeated, it would have been more suitable to introduce a flat section leading up to the terrain surface, while retaining a developed inlet profile.

No mesh convergence study was undertaken due to the high computational expense of simulations. The mesh was deemed of high enough resolution and without the addition of many more cells and a good boundary layer mesh, difficult to reduce y^+ values across the terrain. For stability, and with an increased mesh resolution, the time step would have also have to have been reduced to satisfy a Co of <0.5, increasing the computation time for the solution.

It was shown in the Askervein Hill study, the sensitivity of results to surface roughness and the relationship between actual roughness (vegetation, man-made features) and their definition within OpenFOAM. In this case, an average surface roughness was used, which may have reduced the accuracy of results. Such a problem is inherent in the Richards & Hoxey approach, because k-epsilon parameters are based upon the surface roughness. In future work, a variable surface roughness (and accompanying wall function) could be introduced to provide more accurate parameters for k and ε. This has been performed by Tapia [42] and Azevedo [19] with some success in accurately simulating ABL flow over complex terrain. To further improve results, the use of alternative meshing software is highly recommended in order to effectively add boundary layer cells. This was often the approach taken in literature, with the use of Fluent, CFX or user-developed meshers. Future work in producing accurate studies extends to altering OpenFOAM wall functions. Customised rough wall functions could be used to account for varying rough surfaces, based on original Lidar data and height contours. Vegetation and trees could also be modelled as semi-porous regions near the terrain surface. With improved meshing and y^+ values close to 1, DES could be used to accurately model the ABL and flow over complex terrain. However, these studies would require very high resolution meshes, and have a correspondingly high computational expense.

4.3. *Bridge Deck Results*

Table 4. Comparing lift and drag coefficients to experimental data

Data source (normalised)	Coefficient of drag (C_D)	Coefficient of lift (C_L)	C_D % error	C_L % error
Terrain Inlet	0.096	-0.276	-1.71%	6.58%
Standard Inlet	0.066	-0.252	-32.41%	-2.827%
Experimental [43]	0.098	-0.259	-	-

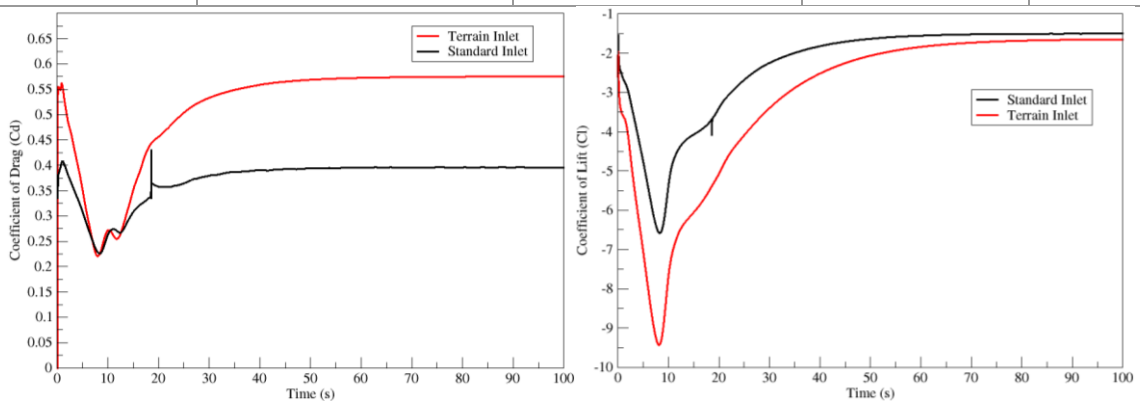

Figure 27. Coefficient of lift and drag for the bridge deck under different inlet conditions

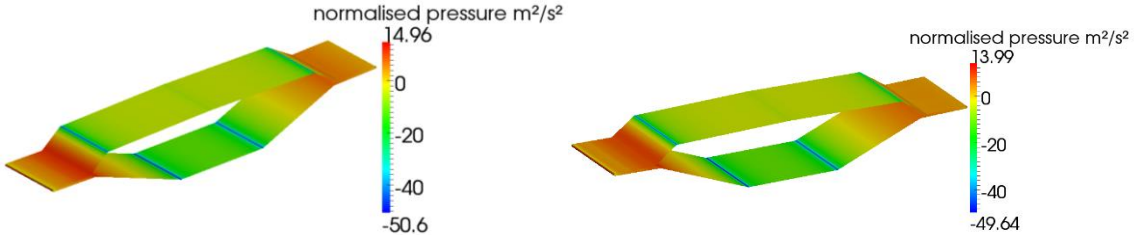

Figure 28. Pressure on bridge deck, terrain inlet (left), standard inlet (right)

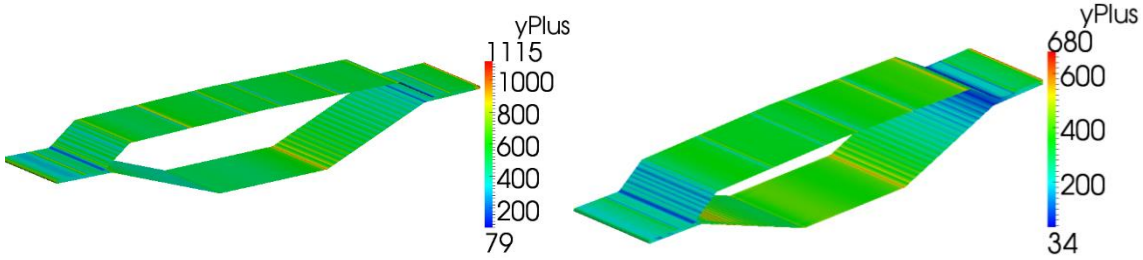

Figure 29. Y^+ values on bridge deck, terrain inlet (left), standard inlet (right)

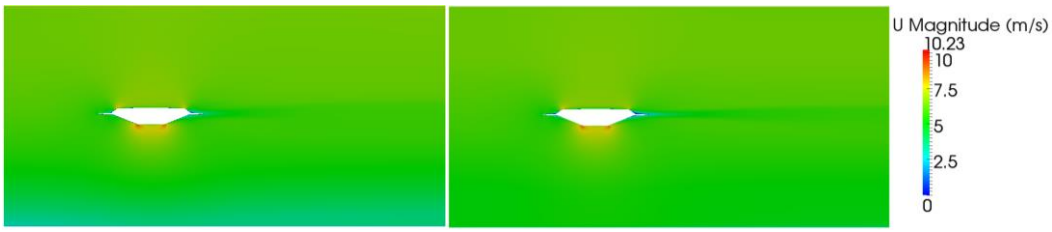

Figure 30. Velocity contour plot for terrain inlet (left), standard inlet (right)

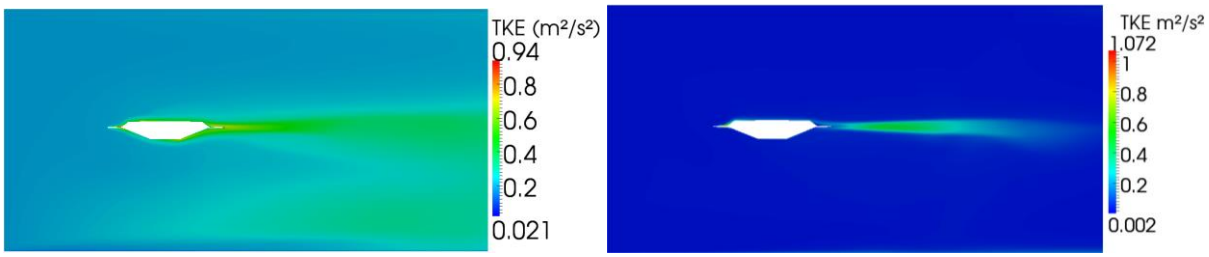

Figure 31. TKE plot for terrain inlet (left), standard inlet (right)

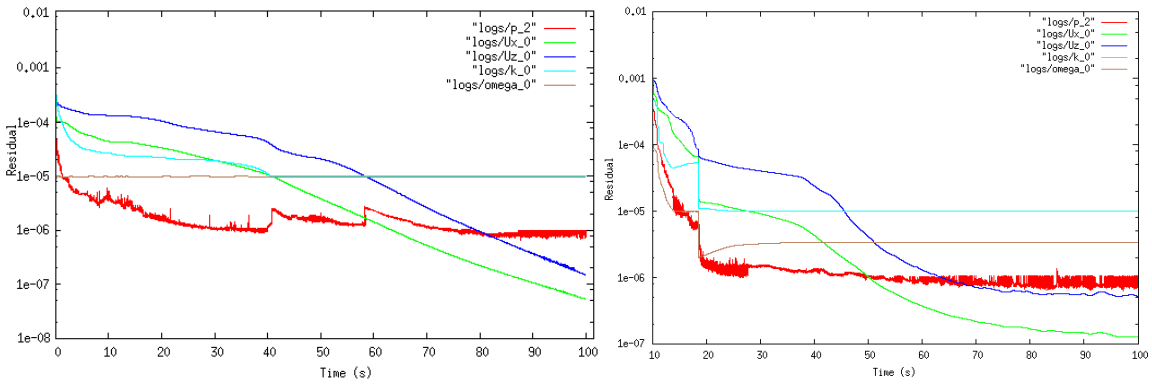

Figure 32. Residuals for deck with terrain inlet (left) and standard inlet (right)

4.3.1. Analysis and Discussion

The results from this simulation, in the form of pressure distributions and forces on the Humber Bridge deck, were supplied to Fieldhouse [2]. This was for the purpose of using them as mean forces for use in modal and harmonic structural analysis finite element models. This case study was produced with the purpose to provide results and data to the structural subgroup, while CFD subgroup DES simulations were running (these took several weeks).

In validating the accuracy of this simulation, calculated coefficients of lift and drag compared well with experimental data (Table 4) [43]. The coefficients were normalised for velocity (multiplied by $0.0016U^2$), and had low percentage errors. Differences can be attributed to numerical error and the simplification of the deck section for CFD analysis (omitting fences, road features). The lift force is negative, showing that the terrain inlet has the effect of adding increased tension to the cables of the Humber Bridge. This demonstrates the sensitivity of the bridge to topographic speed-up, although the profile used was from a point over the most complex terrain near the Humber estuary. With this profile, the total effect across the span of the bridge (2100m) of the terrain inlet at 7m/s, would be a lift force of -17.3kN and a drag force of 6.15kN. This compares to a total lift force of 4.15kN and drag force of -15.78kN at 6.4m/s. Across the span of the bridge, this is a negligible difference. Only very high velocity wind speeds and the resulting topographical speed-up would have a significant impact on the bridge.

With both inlet profiles, most of the y^+ values of the bridge deck were in the region between 30 and 300 (Figure 29). Combined with the use of the k-omegaSST model, this ensured that the boundary layer flow over the bridge deck was accurately modelled. First order divergence schemes were used initially, then central differencing introduced to improve the numerical accuracy of the results.

The key differences between the standard inlet, and the inlet derived from the terrain profile, were in the pressure distributions on the deck (Figure 28) and the distribution of the TKE in the wake (Figure 31). The results of the different inlets were directly comparable, as they used the same computational mesh and differencing schemes. The pressure drop across the deck was slightly higher with the terrain inlet, due to the increased inlet velocity. With the terrain inlet, the turbulent wake was more diffusive than the standard inlet. This may be attributed to the increased inlet velocity, widening the wake due to increase separation of the boundary layer of the deck. To improve the results of this study and for a more accurate result of flow over the bridge deck, the OpenFOAM *mapFields* utility could have been used to transfer all parameters of the flow from the Humber terrain case, directly to the inlet of this case. This would have carried over the turbulent length scale quantities (k, ε) to better represent the flow, rather than just the velocity flow profile.

This study showed that a change in wind flow, due to topography, would have a small effect in pressure distributions and lift and drag forces upon a bridge deck, such as that of the Humber Bridge. At a height of 30m above ground, and in the absence of very complex topography, it is not shown in this case, that these effects would be significant. It would be expected that serious effects, including vortex-induced vibrations or other aeroelastic effects, could take place, if a bridge deck was downstream of significant topographical or man-made features. Future work in this area, could assess the impact of dynamic aeroelastic effects on Bridge decks, over more complex topographical features and structures, which may be influenced by wind funnelling, urban canyon flow and significant topographical wind velocity speed-up.

5. Conclusions

5.1. Conclusions

Presented in this report were three RANS simulations; a case study of flow over the Akservein Hill, to validate initial conditions used in accurately simulating ABL flow over complex terrain,

a case study of ABL flow over terrain near the Humber Bridge, and a case study of flow over the Humber Bridge deck. These studies were performed with the intention of studying the effect that topographic features have on wind flow and the resulting impact this had on a bridge deck.

To accurately simulate flow over terrain two key steps were taken. Accurate terrain geometry in the form of STL files was generated from Lidar data formats. The geometry was meshed using the native OpenFOAM meshing utilities. For correct numerical simulation of the ABL, boundary conditions were used, influenced by the work of Richards & Hoxey [16], and O'Sullivan [38]. In the Askervein case study it was determined that results of wind speed-up and TKE in the flow were very sensitive to the values chosen for the surface roughness of the terrain that the flow was being simulated over. This study also influenced the use of time marching solvers in future simulations of flow over terrain, in order to capture transient effects and accurately model separated flows. Topography near the Humber bridge was determined to have an influence on wind flow, with wind speed-up ranging from -0.325 to 0.15. A flow profile from this case was used as an inlet condition in flow over the Humber Bridge deck. This flow was determined to have an insignificant effect upon a bridge deck, with increases in lift and drag coefficients of 0.03 and -0.024 respectively, when compared to a standard inlet condition. The flow profile generated from the Humber terrain case was used as a mean inlet profile in wider group project CFD simulations.

5.2. Future Work

Future work in this topic should include the adoption of variable surface roughness's and accompanying wall functions for the terrain patches within the fluid domain. These would require adapting wall functions within a chosen CFD solver. Verifying an exact relationship between the actual surface roughness of topographical features (vegetation, man-made structures) and their definition (Ks, Cs) within the CFD code OpenFOAM is also required. To solve the biggest issue of validation, accompanying wind tunnel tests should be undertaken in future studies to determine the numerical errors given by CFD in simulating ABL wind flow over topography. It is important to remember that CFD and wind tunnel testing are both forms of simulation and that results will vary from real world flows. This is particularly the case, as many influencing factors (buoyancy, stratification) are ignored when modelling the ABL. To capture transient effects of velocity and accurately simulate turbulence in the ABL over complex topography, DES is the ideal solver of choice. However, due to the high resolution

meshing requirements and small time step required, simulation of the ABL in this manner would be very computationally expensive.

6. Project Management

6.1. Project Management

Progress in the project was tracked using a Gantt chart (Table 5). A handwritten logbook and Excel were used to record data, sketches, calculations and settings on CFD simulations. The project was divided into a set of work packages, some requiring pre-requisite (critical) work or data. The Gantt chart ensured that deliverables were achieved on time, in accordance with group project objectives. CFD simulations can take days or weeks so a conservative approach was taken in time management. This ensured that time was available to overcome obstacles and enact contingency plans if work packages were delayed. As a research project some work packages changed in both content and duration over the course of the project.

Consideration was given to the length of time simulations took to run. Simulation time depended upon; mesh resolution, turbulence model, time step, differencing schemes, and solvers. 4 and 12 core @ 3.47 GHz processor computers were used. With parallel processing, computation time was reduced. CFD cases were set up during the day and run (unattended) overnight, as practiced in industry. Some high resolution grid simulations took several days to run. Therefore, work packages were planned to be performed concurrently these.

Progress was reviewed at weekly meetings with group members and the project supervisor. Meetings were run by a chair, responsible for circulating an agenda. A secretary recorded minutes and actions for individuals, ensuring accountability for progress and deliverables. Roles were rotated between the CFD and structural subgroup members. Agendas, minutes, data, research articles, models and reports were shared through cloud based storage, Dropbox.

Table 5. Project Gantt chart

Task	Week	Term 2												Easter			
		1	2	3	4	5	6	7	8	9	10	11	12	1	2	3	4
	Converting Lidar data in STL format					x											
	Case of bridge deck with terrain domain																
	Literature study for validation cases																
	Produce case study of the Askervein Hill								x								
	Define approach for future case studies and ABL boundary layer flow																
	Setup case for Humber Bridge terrain flow using topographical data											x					
	Integrate results into study of flow over bridge deck																
	Compare results and provide data to Fieldhouse for analysis																
	Set up mesh for group DES case and run													x			
	Obtain results, compare to structural subgroup																x
	Collaborate group and sub group results and provide final recommendations																
	Writing I2 and G2																x

Key	
Person/Group	Colour
JM	
As part of CFD sub-group	
Milestones	x
Cutoff to run DES modelling	

6.2. Project Risk Assessment

Project risk assessment was comprised of health and safety risk management and strategies to mitigate risk for project deliverables (Table 6). All work in this project took place using a computer so a University of Exeter display screen equipment self-assessment form was completed [44]. A score of 12 was calculated, showing that the computer workstations used were suitable and safe for prolonged use.

Table 6. Project risk assessment criteria and mitigation strategies for deliverables

Risk item	Effect	Cause	Likelihood /10	Severity /10	Importance L*S	How risk was mitigated
Unable to import terrain data to OpenFOAM or CAD in correct file format (.stl).	No analysis of wind flow over topography.	High cost of data conversion software.	3	10	30	Use of MeshLab and GlobalMapper.
Unable to mesh the flow domain appropriately.	Incomplete analysis.	Poor quality .stl imports.	3	8	24	Use of digital elevation models.
Unable to validate CFD data with experimental data.	Lack of accuracy and reliability in results.	Lack of experimental data.	1	5	5	Created Askervein hill validation case.
Failure to complete LES simulations.	Lack of results for comparison to structural subgroup.	LES high meshing requirements.	3	5	15	Group work on DES case. Use of Callisto HPC.

6.3. Project Cost and Sustainability Considerations

A consideration of this project in terms of research, was its transferability to a commercial environment. Costs were low, because the Lidar data required was free for academic use and open source software (OpenFOAM, MeshLab) was used. Table 7 compares approximate costs between CFD analysis and the industry standard for wind engineering, BLWT testing. While CFD cannot produce the same quantity of data as a BLWT test it may be useful for specific cases of analysis and design. In terms of sustainability, different flows and terrain were simulated and the results used to predict the effect of wind flow without having to use wind tunnel testing. This saved material usage and the high cost of running a large wind tunnel. By predicting the effects of wind flow on terrain and the resulting response of a bridge deck, long span bridges may be built more efficiently. This would reduce the use of energy intensive materials (steel and concrete), and production of CO_2 and pollution. Given the reducing cost of HPC processors and increasing processor speeds, CFD simulation is a sustainable method for analysis, particularly with licence-free software such as OpenFOAM.

Table 7. Costs associated with Project

Details	Commercial Cost
Lidar data for CFD: Humber Bridge terrain: 84 grid squares, 83.98km^2.	£7535.53
Software Licence: GlobalMapper, (GIS software).	£275.00
BLWT testing: Single day of full aeroelastic model testing at multiple angles of wind flow attack.	£25,000-£30,000[45]

7. Contribution to Group Functioning

7.1. CFD Subgroup

Most of the contribution to the project took place within the CFD subgroup. Feasibility in combining both terrain and a bridge deck into LES or DES studies was established in this report. These numerical methods were required to determine frequency of vortex shedding from the Humber Bridge deck. Given the impractically high mesh resolution requirements this approach was abandoned. A different approach was taken to include the effect of topography through implicit means. A mean velocity profile was derived from simulations of flow over terrain near the Humber Bridge. These were given to Richmond [2] who applied the profile with a superimposed fluctuating turbulence as an inlet condition in DES subgroup simulations of ABL flow over the Humber Bridge deck. For this case, an initial SHM was set up by the author, although meshing was undertaken as part of a group effort. A mesh was also made on Pointwise (Figure 33). Ultimately the mesh was not used in the final simulations due to the slow turnaround time in altering the mesh in respect to post-processed y^+ values. A cost analysis of CFD and BLWT testing was made to determine if the group methodology was practical and competitive in a commercial environment.

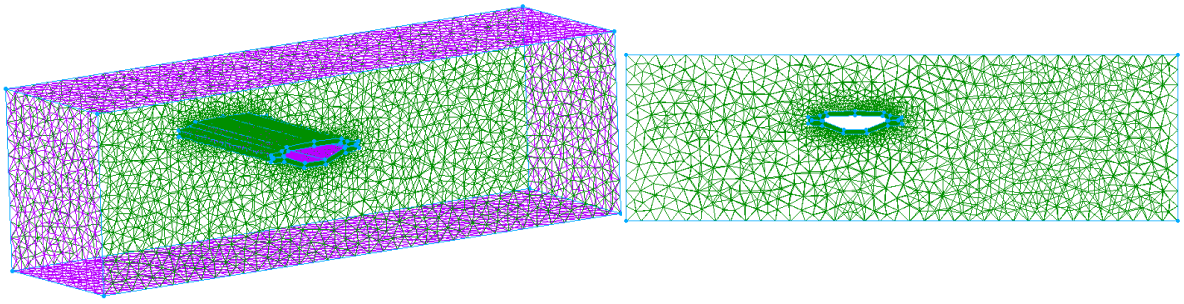

Figure 33. Structured boundary layer and unstructured tetrahedral mesh of Humber Bridge deck constructed on pointwise

7.2. Fluid-Structure Interaction

The vibrational modes and natural frequencies are dependent upon the design of the Humber Bridge. The structural subgroup determined the natural frequencies of a simplified bridge deck while the CFD subgroup made efforts to determine the natural rate of vortex shedding by the bridge deck acting as a bluff (non-aerodynamic) body. The author supplied mean surface pressure distributions and forces upon the Humber Bridge deck to Fieldhouse [2] for application in determining the vibrational response of the deck. CAD drawings of the Humber Bridge were constructed in SolidWorks by Fieldhouse, and provided for analysis in this project. The CAD models were simplified in this report for CFD analysis by removing fillets and additional features, and the deck scaled up to an appropriate size.

8. References

[1] Fujino, Y. Siringoringo, D. (2013) 'Vibration mechanisms and controls of long-span bridges: A review', *Structural Engineering International*, 23(3), pp. 248-268.

[2] Fieldhouse, D. Lambton, P. Morgan, J. Mullins, J. Richmond, J. Jiménez, V.T. (2015) *Research into the causes and effects of Aeroelastic flutter on long span bridge structures (Report)*, Exeter, UK: Authors.

[3] OpenFOAM Foundation, OpenFOAM (Version 2.1.0) [Open Source CFD code]. Available at: *http://www.openfoam.com/* (Accessed: 28th April 2015).

[4] Marjanovic, N. Wharton, S. Chow, F.K. (2014) 'Investigation of model parameters for high-resolution wind energy forecasting: Case studies over simple and complex terrain', *Journal of Wind Engineering and Industrial Aerodynamics*, 134(1), pp. 10-24.

[5] Mullins, J. (2014) *Topographical and Environmental Effects on Fluid Flow using Computational Techniques (Report)*, Exeter, UK: Mullins, J.

[6] McAuliffe, R. Larose, G.L. (2012) 'Reynolds-number and surface-modeling sensitivities for experimental simulation of flow over complex topography', *Journal of Wind Engineering and Industrial Aerodynamics*, 104-106(1), pp. 603-613.

[7] Linfield, K. Mundry, R.G. (2014) *Pros and Cons of CFD and Physical Flow Modelling (White Paper)*, Liviona, MI, USA: Airflow Sciences Corporation.

[8] Roberts, S. (2013) *Wind Wizard: Alan G. Davenport and the Art of Wind Engineering*, Princeton, N.J, USA: Princeton University Press.

[9] Davenport, A.G. King, J.P.C. (1990) 'The influence of topography on the dynamic wind loading of long span bridges', *Journal of Wind Engineering and Industrial Aerodynamics,* 36(2), pp. 1373-1382.

[10] Moon, K. Hwang, J. Kim, B-G. Lee, C. Choi, J. (2014) 'Large-eddy simulation of turbulent flow and dispersion over a complex urban street canyon', *Environmental Fluid Mechanics,* 14(6), pp. 1381-1403.

[11] Paterson, D.A. Holmes, J.D. (1993) 'Computation of wind flow over topography', *Journal of Wind Engineering and Industrial Aerodynamics,* 46-47(1), pp. 471-476.

[12] Geomatics-Group. Environment Agency. (2015) *Lidar Data,* Available at: *https://www.geomatics-group.co.uk/geocms/* (Accessed: 29th March 2015).

[13] Bechmann, A. Berg, J. Courtney, M.S. Jorgensen, H.E. Mann, J. Sorensen, N.N. (2009) *The Bolund Experiment: Overview and Background*, Denmark: Riso National Laboratory.

[14] Taylor, P.A. Teunissen, H.W. (1983) *The Askervein Hill Project: Report on the Sept./Oct. 1983, Main Field Experiment, Research Report MSRB-84-6 (Technical Report),* Ontario, Canada: Meteorological Services Research Branch Atmospheric Environment Service.

[15] Peralta, C. Nugesse, H. Kokilavani, S.P. Schmidt, J. Stoevesandt, B. (2014) 'Validation of the simpleFoam (RANS) solver for the atmospheric boundary layer in complex terrain', *First Symposium on OpenFOAM in Wind Energy,* 2(1), pp. 1-10.

[16] Richards, H. Hoxey, R. (1993) 'Appropriate boundary conditions for computational wind engineering models using the k-e turbulence model', *Journal of Wind Engineering and Industrial Aerodynamics,* 46-47(1), pp. 145-153.

[17] Gobbi, M.F. Dorweiler, R.P. (2012) 'Simulation of wind over a relatively complex topography: application to the Askervein Hill', *Journal of the Brazilian Society of Mechanical Sciences and Engineering,* 34(4), pp. 492-500.

[18] Castro, F.A. Palma, J.M.L.M, Silva Lopes, A. (2003) 'Simulation of the Askervein Flow. Part 1: Reynolds Averaged Navier-Stokes Equations (k-e Turbulence Model)', *Boundary Layer Meteorology,* 107(1), pp. 501-530.

[19] Azevedo, J.M.S. (2013) *Development of procedures for the simulation of atmospheric flows over complex terrain, using OpenFOAM (Master's Thesis),* Porto: Polytechnic of Porto.

[20] Silva Lopes, A.S. Palma, J.M.L.M. Castro, F.A. (2007) 'Simulation of the Askervein flow. Part 2: Large-eddy simulations', *Boundary-layer Meteorology,* 125(1), pp. 85-108.

[21] Bechmann, A. Sorensen, N.N. Johansen, J. (2007) *Atmospheric Flow over Terrain using Hybrid RANS/LES*, Denmark: Wind Energy Department, Riso National Laboratory.

[22] Richards, P.J. Norris, S.E. (2011) 'Appropriate boundary conditions for computational wind engineering models revisited', *Journal of Wind Engineering and Industrial Aerodynamics*, 99(1), pp. 257-266.

[23] O'Sullivan, J.P. Pecnik, R. Iaccarino. G. (2010) *Investigating turbulence in wind flow over complex terrain*, pp. 129-139. Proceedings of the Summer Program 2010: Center for Turbulence Research, Stanford University.

[24] Bakker, Andre. (2002) *Applied Computational Fluid Dynamics*, Fluent Inc.

[25] Krogstad, P.A. Antonia, R.A. (1999) 'Surface roughness effects in turbulent boundary layers', *Experiments in Fluids*, 1999(27), pp. 450-460.

[26] Tu, J. Yeoh, G. H. Liu, C. (2007) *Computational Fluid Dynamics: A Practical Approach*, 2nd edn. United Kingdom: Butterworth-Heinemann.

[27] Breuer, M. Jovicic, N. Mazaev, K. (2003) 'Comparison of DES, RANS and LES for the separated flow around a flat plate at high incidence', *Numerical Methods In Fluids*, 41(4), pp. 357-388.

[28] Wilcox, D.C. (1993) *Turbulence Modeling for CFD*, 2nd edn. California: DCW Industries.

[29] Cfd Online (2015) *Law of the wall*, Available at: *http://www.cfd-online.com/Wiki/Law_of_the_wall* (Accessed: 27th April 2015).

[30] Frei, W. (2013) *Turbulence Modelling*, Available at: *http://www.comsol.com/blogs/which-turbulence-model-should-choose-cfd-application/* (Accessed: 27th April 2015).

[31] Stevens, A. (2008) *ascii2xyz*, Available at: *http://uk.mathworks.com/matlabcentral /fileexchange/21785-ascii2xyz/content/ascii2xyz.m* (Accessed: 27th April 2015).

[32] Holdaway, D. Tabor, G. Beare, B. (2007) *An Examination of the Feasibility of Using OpenFOAM to Model Air Flow for Wind Turbine Positioning*, Exeter, UK: University of Exeter.

[33] Avila, M. Owen, H. Folch, A. Prieto, L. Cosculluela, L. (2015) 'Wind modelling over complex terrain using CFD', *Geophysical Research Abstracts*, 17(1), pp. 1-3.

[34] Franke, J. Hellsten, A. Schlunzen, H. Carissimo, B. (COST) (2007) *Best Practice Guideline for the CFD Simulation of Flows in the Urban Environment. COST Action 732*, Hamburg, Germany: University of Hamburg, Meteorological Institute.

[35] Blocken, B. Stathopoulos, T. Carmeliet, J. (2007) 'CFD simulation of the atmospheric boundary layer: wall function problems', *Atmospheric Environment,* 41(2), pp. 238-252.

[36] Yang, Y. Gu, M. Chen, S. Jin, X. (2009) 'New inflow boundary conditions for modelling the neutral equilibrium atmospheric boundary layer in computational wind engineering', *Journal of Wind Engineering and Industrial Aerodynamics,* 97(1), pp. 88-95.

[37] O'Sullivan, J.P. Archer, R.A. Flay, R.G.J. (2011) 'Consistent conditions for flows with the atmospheric boundary layer', *Journal of Wind Engineering and Industrial Aerodynamics,* 99(1), pp. 65-77.

[38] O'Sullivan, J. (2012) *Modelling Wind Flow over Complex Terrain (PhD Thesis),* Auckland, New Zealand: The University of Auckland.

[39] World Meteorological Organization (2008) *Guide to Meteorological Instruments and Methods of Observation*, 7th edn, pp 132. Geneva, Switzerland: WMO.

[40] Stangroom, P. (2004) *CFD Modelling of Wind Flow (PhD Thesis)*, Nottingham, UK: The University of Nottingham.

[41] Met Office (2014) *UK Wind Map Issue 1. Setting the standards for site search for small and medium wind projects*, Exeter, UK: Met Office.

[42] Tapia, X.P. (2009) *Modelling of wind flow over complex terrain using OpenFoam (Master's Thesis)*, Gavle, Sweden: University of Gavle.

[43] Walshe, D.E. Cowdrey, C.F. (1972) *A Further Aerodynamic Investigation For The Proposed Humber Suspension Bridge*, Teddington, UK: National Physical Laboratory.

[44] University of Exeter, 2014. *Health and Safety Standard: DSE and Portable Workstations.* Available at:*http://intranet.exeter.ac.uk/emps/healthandsafety/collegespecificsafetystandards/displayscreenequipment/* (Accessed: 29th April 2015).

[45] Correspondence with J. Tearle, Structural Engineer, Ramboll, UK. [Email] 23/03/2015.